HHS Public Access

Author manuscript

Nat Rev Cancer. Author manuscript; available in PMC 2024 March 01.

Published in final edited form as:

Nat Rev Cancer. 2023 September ; 23(9): 581–599. doi:10.1038/s41568-023-00593-3.

Micro- and nano- engineering approaches to investigate tumour ecosystems

Mijin Kim[1], **Magdalini Panagiotakopoulou**[1], **Chen Chen**[1,2,3], **Stephen Ruiz**[1,2], **Karuna Ganesh**[1,2], **Tuomas Tammela**[2,4], **Daniel A. Heller**[1,2,*]

[1]Molecular Pharmacology Program, Sloan Kettering Institute, New York, NY,United States

[2]Graduate School of Medical Sciences, Weill Cornell Medicine, New York, NY,United States

[3]Tri-institutional PhD Program in Chemical Biology, Sloan Kettering Institute, New York, NY,United States

[4]Cancer Biology & Genetics Program, Sloan Kettering Institute, New York, NY,United States

Abstract

The interactions between tumour cells, the tumour microenvironment (TME), and non-tumour tissues are of interest to many cancer researchers. Micro-engineering approaches and nanotechnologies are under extensive exploration for modelling these interactions and measuring them *in situ* and *in vivo* to investigate therapeutic vulnerabilities in cancer and extend a systemic view of tumour ecosystems. Herein, we highlight the greatest opportunities for improving the understanding of tumour ecosystems using microfluidic devices, bioprinting, or organ-on-a-chip approaches. We also discuss the potential of nanosensors that can transmit information from within the TME or elsewhere in the body to address scientific and clinical questions about changes in chemical gradients, enzymatic activities, metabolic- and immune profiles of the TME and circulating analytes. This review aims to connect the cancer biology and engineering communities, presenting biomedical technologies that may expand the methodologies of the former, while inspiring the latter to develop approaches for interrogating cancer ecosystems.

TOC Blurb:

Tumour ecosystems encompass a multitute of variables, including enzymatic, metabolic, and immune components within the tumour and across organs. This Review summarizes how microengineering approaches and nanosensors have been used to establish multicomponent tumour models and to assess tumour plasticity.

* hellerd@mskcc.org .

Author contributions

M.K., M.P., C.C. and S.B.R. researched data for the article. M.K., M.P., C.C., K.G., T.T. and D.A.H. contributed substantially to discussion of the content. M.K., M.P., C.C. and S.B.R. and D.A.H wrote the article. M.K., K.G., T.T. and D.A.H reviewed and/or edited the manuscript before submission.

Introduction

The tumour ecosystem comprises molecular and cellular interactions between tumour cells, the tumour microenvironment (TME), and other organs or tissues.[1–4] Appreciating these interactions is crucial for understanding tumourigenesis and tumour progression.[3–6] Tumour cells survive and proliferate in extreme cellular environments, subject to conditions such as hypoxia **[G]**, acidosis, nutrient deficiency, and immunoediting **[G]**.[4,6–8] Cellular and molecular crosstalk in tumour ecosystems is linked to every stage of tumour growth, invasion, and metastasis.[9] Therefore, understanding the spatial and temporal complexities of signaling and metabolic pathways, secreted factors, extracellular matrix (ECM) components and the immune compartment of the TME is crucial for determining the drivers of tumour progression and for identifying potential therapeutic interventions. Although biochemical and omics-based approaches have been conventionally used to study the tumour ecosystem, improved measurement technologies and tumour ecosystem modeling through micro- and nanoscale engineering can help deconvolute these studies. For example, tracking biomarker and metabolic profiles dynamically *in situ*, yields an extra level of spatial information about the TME that can provide novel biological insights. Micro- and nanoscale engineering utilizes innovative systems and designs at small dimensions to either recapitulate the TME or provide spatiotemporal reporting of biochemical signals.

With this Review, we aim to connect the cancer biology and engineering communities, stimulating closer collaboration among them for expanding current toolsets to address open questions about cancer ecosystems. We first review available micro- and nanoscale engineering approaches and discuss how they can be implemented to recapitulate complex and dynamic molecular, cellular, and systemic components of the TME by incorporating various chemical gradients, ECM-mimicking structures, signalling and metabolic components, and cell types into models. Next, we discuss the development of bioimaging and sensing probes that can help monitor molecular and cellular crosstalk and detect biomarkers *in situ* and *in vivo*. Finally, we discuss roadblocks hindering the broad use of engineered tools and opportunities for addressing outstanding questions on tumour ecosystems.

Engineering approaches for cancer research

Developments in micro- and nanotechnologies and related engineering approaches have advanced toward basic and translational research applications (Table 1). Microscale technologies find wide applications in high-throughput screening and structural fabrication. For example, microfluidic systems **[G]** have been developed for high-throughput single-cell analysis to investigate potential therapeutic vulnerabilities.[10] Tumour models with **self-assembled microvessels** [G] have been used to recapitulate disease pathophysiology in pharmacological testing.[11] Multi-organ chips comprised of engineered tissues linked by vascular flow enable the study of cytokine-mediated communication, circulating cells, and exosomes, and to assess clinical pharmacokinetic and pharmacodynamic profiles of drugs and toxicity biomarkers.[12] Microscale bioprinting can incorporate perfusable blood vessel networks into 3D tumour models to mimic in vivo cellular heterogeneity, cell-cell interactions, and spatial tomography, to predict therapy responses.[13] Nanoscale approaches

leverage molecular interactions on nanometer-sized materials to generate precise responses for an analyte of interest. Optical, magnetic, and radiolabelled nanoparticles are used as sensing materials for cancer biomarkers and diagnosis[14], scavenging platforms to enrich and isolate cancer-derived analytes for omics analysis,[15] and in vivo tumour imaging[16] (Table 2). Several promising micro- and nanoengineered technologies are approved or under clinical investigation to improve outcomes in cancer patients (Box 1).

While the translational potential of micro- and nano-engineering approaches has been widely investigated, many existing, promising engineering technologies have not yet been deployed in cancer research. Opportunities exist for the use of these technologies in extending a systemic view of tumour ecosystems. Since bioengineered tumour models can mimic TME features, they exhibit promise for studying metastasis and the mechanisms of tumour growth, as well as drug toxicity and therapeutic efficacy. Nanoengineered sensing materials and measurement techniques can be employed to temporally and quantitatively monitor subtle changes in targets of interest in live cells and in vivo, enabling mechanistic investigations of biological processes and leading to new drug targets.

Engineering of tumour models

All stages of cancer research, from mechanism and biomarker discovery to translational and clinical research, require the development of preclinical models that approximate aspects of tumour ecosystems. These range from conventional two-dimensional (2D) cell culture systems to multicellular spheroids[17] **[G]**, organoids **[G]**, and mouse models (Figure 1). Conventional 2D culture systems of cancer cell lines lack the geometrical and biological complexity of the TME, and suffer from genetic drift **[G]** and bottleneck effects **[G]** due to long-term maintenance *in vitro*.[18] Moreover, spheroid or organoid cultures usually lack microenvironmental components, and differences in research protocols can result in heterogeneity.[19] Encouraging steps are being taken to optimize and standardize 3D cell culture conditions and introduce microenvironmental components.[20,21] Both 2D and 3D culture systems are static, where the dynamic, flow-related biophysical, and physiological conditions of the ecosystem cannot easily be reproduced. 3D bioprinted cancer models incorporate perfusable vessels, different modular cell types with controlled organization, and an ECM within the model, recapitulating tissue plasticity or stromal cell epigenetic modifications induced by the tumours.[22,23] However, the complex architectures of 3D bioprinted cancer models require expensive equipment and highly trained interdisciplinary teams.

Mouse tumour xenograft models **[G]** comprise the use of immunocompromised mice transplanted with human patient-derived xenografts (PDXs) or cell-derived xenografts(CDXs), genetically-engineered mouse models (GEMMs), or environmentally-induced tumour mouse models. PDX mouse models, where patient tumour cells are transplanted into immunocompromised mice, either orthotopically or heterotopically, have been used to model therapeutic drug responses in patients with high accuracy.[24] However, the absence of the immune component hampers their application for the development and testing of immunotherapies.[25] In GEMMs, the genomes of mice are altered such that one or several genes involved in carcinogenesis or tumour progression are mutated, deleted, or

overexpressed; subsequently, the effects of such genetic modifications on autochthonous tumour development and responses to therapies can be investigated over time. GEMMs involve immunocompetent mice that better reflect the TME than PDX models. However, in GEMMs, a limited number of genes are typically modified, which is not reflective of the mutational landscapes observed in human cancer cells. Recent developments in somatic engineering of cancer genomes in vivo are rapidly reducing the cost and time required for GEMM generation and enabling the development of more complex models.[26] Finally, carcinogen-induced tumour models, such as ultraviolet B (UVB)-induced skin cancer, offer greater genome instability than GEMMS that better reflects tumourigenesis in humans, but the models are rarely used due to genetic complexity, considerable variation in progression, and the limited number of cancers that can be modeled.[27] Murine models present a more comprehensive TME picture than in vitro models. However, challenges remain in high cost and time for model development, ethical concerns, and deconvolution of the TME networks.

Micro- and nano-engineering approaches to mimic the TME can augment the physiological relevance and complexity of the currently available tumour models. They can facilitate aspects such as spatially defined co-cultures, confined cell migration, systematically controlled nutrient or hypoxia gradients, shear stress, and traction forces (Figure 2). Such engineered models range from static culture systems with spatial features of controlled geometry and mechanical properties such as electrospun nanofibers **[G]**,[28,29] nanoprinted scaffolds **[G]**,[30,31] to systems incorporating dynamic physiological features into both nano- and micro-structure substrates[32]. Static engineered microenvironments such as microcontact printed lines **[G]** allow for the decoupled study of factors that influence cancer cell migration, including confinement size, substrate stiffness, ligand density, and the effect of external gradients.[33,34] These in vitro models provide a simplified approach to the in vivo setting and enable the well-controlled modulation of the microenvironment to investigate cell shape, protein activation, actin polymerization,[35–38] and the effects of chemical gradients on cell migration.[39] Furthermore, tumour-on-a-chip (ToC) devices are microfabricated cell cultures that combine the advantages of microfluidic technology and 3D cell culture technology to mimic the complexity and characteristics of native organs.[40–43] Microfluidic devices can reconstruct dynamic physiological characteristics in tissues, such as fluidic flow, shear stress and tension, and nutrient delivery.[44–47] Spatiotemporal dynamics of biological processes in the TME can be assessed by high-resolution real-time imaging of nanoengineered ToC platforms. In ToC platforms, the tissue height is well-defined and typically sub-millimeter in thickness, making quantitative investigation of key TME parameters, including cell interactions, in live systems easiler compared to traditional 3D in vitro models, like primary cancer organoids[48]. Below, we describe how engineered platforms are used to recapitulate the pivotal structural and functional characteristics of the TME.

Oxygen and chemokine gradients

Hypoxia occurs within the TME due to abnormal blood vessel formation, impaired blood flow and, therefore, decreased oxygen supply caused by rapid tumour growth. Such oxygen level gradients can be reproduced within the microscale dimensions of ToCs. While pericellular oxygen conditions are not possible to control in traditional hypoxia chambers,[49] oxygen gradients can be systematically modeled in various ways: by engineering physical

barriers made of polymers that limit oxygen diffusion through them to generate oxygen gradients[50]; by incorporating tumour spheroids to naturally establish a hypoxic core[51]; or by placing the entire microfluidic chip inside a hypoxia chamber.[52] Other ToC models employ flanking channels filled with oxygen-supplying and oxygen-scavenging medium (such as sodium sulfite) to create a precise gradient across the tissue compartment,[53] for example, to reproduce tumour growth and migratory behavior in response to hypoxia inducible factor 1a (HIF1a) expression as a result of the low oxygen levels (that is oxygen concentrations of less than 5%).[54]

Similarly to oxygen gradients, microfluidic approaches can be used to generate precisely controlled levels of chemokines **[G]**.[55,56] Microfluidic chips have been used to study immune and cancer cell interactions by using chemokine-guided migration assays to investigate how macrophages induce cancer cell migration[57,58] and how pre-activated natural killer (NK) cells migrate towards cancer cells.[59] Gradient control in 3D scaffolds has been employed to study endothelial sprouting in response to vascular endothelial growth factor (VEGF) gradients,[54] to assess directed migration of cancer cells or sprouting of spheroids,[60] to conduct chemotherapeutic screening of different anti-cancer drugs,[61] and to investigate chemokine-guided immune cell migration into the TME.[56,62,63]

The precise control of oxygen, nutrient, and chemokine gradients in microfluidic chips facilitates the study of cancer cell behavior under hypoxia, nutrient deficiency, or other chemical stimuli (e.g., drug resistance) (Fig. 2a–c).

Structural components of the TME

Cell migration is a crucial step in metastasis. Cancer cells migrate by moving through pre-existing paths that are defined by anatomical structures,[64,65] or through paths that have been newly-created, either via ECM remodeling,[66,67] or through the previous migration of cancer-associated stromal cells or ‘leader’ cells.[68] However, TME heterogeneity and the diversity of migration mechanisms of cancer cells complicate the effort to model cancer cell migration under physiological conditions. Specifically, conventional 2D culture systems and cell cultures with ECM gels cannot reproduce the complexity of the TME.[69] To this end, various assays presenting channel-like and fiber-like tracks of defined dimensions and stiffness have been developed to study confined migration (Fig. 2d,g).

Engineering of 3D cell culture scaffolds allows for investigation of the effect of stiffness, porosity, and ECM composition on the migratory behavior of immune cells into the tumour site, of the viability of cancer cells, and of cancer cell growth. Various ECM stiffness can be patterned in situ to mimic different characteristics of solid tumours. For instance, a UV-crosslinkable gelatin methacryloyl hydrogel can generate a tailored ECM with stiffness and porosity that resemble the properties of multiple cancer matrices.[50] Moreover, microfluidic hydrogel models have been used to evaluate correlations between immune cell cytotoxicity and obstruction of migration.[50,70] Interstitial fluid flow and hydraulic resistance are tumour-associated biophysical factors that promote tumour growth and macrophage migration in the TME. ToC models can mimic these events by fluidic perfusion of the TME.[62,71] Such ToC platforms can be imaged to quantify the speed and direction of immune or cancer cell migration[62,72,73] and to uncover specific cell–cell interactions between heterotypic cell

populations[11]. ToCs may not only incorporate multiple cell types into a 3D environment but also integrate a vascular-like flow component.[22,74–78] 2D and 3D micro- and nanostructured features such as arrays of nanopillars or quantum dot nanodiscs have been employed as culture substrates to investigate physical forces between cancer cells and their environment, which govern a number of functional processes such as cell adhesion, cell migration, cell signalling, mechanotransduction **[G]** and ion channel regulation.[79,80] Cell traction forces can be quantitatively assessed via traction force microscopy platforms that optically map deformations on nano- or micro-patterned elastic substrates[79,81,82].

Studying cancer cell behaviour on micro- or nano-engineered surfaces offer a unique capability to decipher the role of different structural elements of the TME in cell growth and migration.

Cellular and tissue components of the TME

Tissue morphology can be recapitulated in 3D cell culture models using porous 3D scaffolds, on which tumour cells can be co-cultured with fibroblasts. For instance, a lung-on-a-chip model was constructed using a porous, nanofiber membrane made of polylactic acid-glycolic acid (PLGA) via electrospinning. On this porous nanofiber membrane, which resembled the alveolar respiratory membrane, human non-small cell lung cancer cells (A549 cells) were co-cultured with human fetal lung fibroblasts (HFL1) and human umbilical vein endothelial cells (HUVECs) to investigate tumor invasion and resistance to the epidermal growth factor receptor (EGFR)-targeting drug gefitinib **[G]**.[76] In this model, cancer cells induced endothelial cell death prior to cancer cell invasion. Co-culture with HFL1 revealed the drug resistance mechanism of A549 cells: Insulin growth factor 1 (IGF1) secretion by the fibroblasts activated the PI3K/Akt pathway in A549 cells to promote resistance to gefitinib.[76] The particular architecture of this lung chip enabled the in vitro induction of alveolar biochemical factors that contributed to tumor invasion and drug resistance.

Spatial orientation of cells and cell type composition can be tailored to mimic various physiological conditions. For example, immune- and cancer cell compositions could be controlled to mimic different types of tumour–immune cell interactions, ranging from interactions found at early-stage tumours, in which only a few cytotoxic lymphocytes are located in the periphery to fully infiltrated tumours.[74] Moreover, the ratio of cancer cells to fibroblasts, immune cells, and endothelial cells could be tuned in a microfluidic chip to assess the antagonistic immunomodulatory effect of cancer-associated fibroblasts (CAFs) via single-cell tracking and quantification of cell–cell interactions.[75] Spatiotemporal imaging of ToC platforms provides insights regarding tumour–immune cell interactions and a platform for assessing cellular therapies and other anti-cancer drugs in real-time, which is otherwise challenging to achieve (Fig. 2f).

Besides original cell co-culture models, organoids and spheroids can be integrated into chips providing, for example, in vitro alternatives to conventional murine in vivo metastasis assays.[77,78] Spheroids-on-a-chip offer both the advantages of spheroid cultures (3D arrangements, cell type, and genomic diversity) and ToC platforms.

Multicellular and multitissue ToCs expand toolset for studying TME from the molecular to the organ level. Precise spatial arrangement of different cells within those platforms (for example, via robotic single-cell manipulation systems) can enable the formation of even more physiologically realistic complex architectures that are now not feasible.

Vasculature and perfusion

Blood and lymphatic vasculatures are crucial components of the TME because they facilitate delivery of oxygen, nutrients, and hormones that directly affect tumour behavior and growth, and just as importantly, dictate response to therapies via the mechanisms of immunevasion and subversion of T cell-mediated immunosurveillance.[7,83] While conventional cell cultures fail to mimic shear stress conditions resulting from interstitial fluid or blood flow, microfluidic systems can be used to recapitulate their physiological and rheological properties by integrating vasculature-like perfusion and channels (Fig. 2e). By incorporating planar monolayers, vascular lumen **[G]**, self-assembled microvessels, and/or endothelial cells into their ToC models, several studies mimicked in vivo-like nutrient or drug delivery to the surrounding tissue.[84,85] Additionally, integration of rheological features of perfusion into in vitro tumour models can help mimic the continuous nutrient delivery and removal of metabolic waste from the TME[86], the culture of cells under vascular intraluminal flow can help model their migratory behavior inside the TME under interstitial flow[62], and the integration of lymphatic and blood vasculatures into multiorgan chips to study off-target toxicities and pharmacokinetics of drugs (Fig. 2h).[87]

High-resolution live-cell imaging in self-assembled microvessels revealed the dynamic roles of inflamed neutrophils in promoting extravasation of cancer cells through the formation of intraluminal clusters of neutrophils and cancer cells.[11] Performing real-time imaging while perfusing provides the opportunity to concomitantly test the perfused media and analyze the kinetics of secreted factors like cytokines **[G]** and the state of circulating tumour cells with temporal resolution.[11]

The heterogeneous tumour microenvironment can also be reconstructed by 3D bioprinting using patient-derived cells, including glioblastoma cells, astrocytes, and microglia.[13,78,88] For example, perfusable blood vessels were created using a sacrificial bioink **[G]** coated with brain pericytes and endothelial cells.[13] Glioblastoma cells in this 3D bioprinted tumour model showed similar growth curves, drug responses, and genetic signatures as in orthotopic transplantation models. Vascularization and perfusion in ToC models recapitulate nutrient delivery and shear stress conditions in the TME. Construction of dimensional and cellular hierarchies and reproduction of molecular and cellular heterogeneity in vascular networks remain challenging.[89] Development of new bioinks, and the combination of bioprinting technologies with traditional nanolithography **[G]** tools will improve engineering the complexity of vascular networks in ToCs.

To summarize, incorporation of diverse engineering approaches with micro- or nanoscale resolution into tumour models enables recapitulation of complex tumour ecosystems at a molecular, cellular, tissue, and systemic level. Such engineering approaches assist studies on cancer cell invasion and dissemination and provide the opportunity to assess drug efficacy

in vitro with improved clinical relevance. In the next section, we discuss nanoscale analytic technologies to investigate tumour ecosystems in live cells and in vivo.

Probing tumour ecosystems

Hypoxia, acidosis, and nutrient deficiency make the TME a hostile environment for cellular proliferation.[4,6] The complex metabolic interplay and communication between tumour cells, the TME, and distal organs orchestrate ever-evolving ecosystems for tumour initiation, expansion, and metastasis. (Figure 2).[5] The measurement of spatiotemporal information as conferred by the levels of biomarkers and metabolites in tumour ecosystems is important because the functions and interactions of tumour cells are highly time- and location-dependent.[1,2,90,91] Challenges remain in studying cancer metabolism, including measurement of the metabolic crosstalk, both within the TME and systemically, and in assessing responses to genetic or therapeutic interventions.[9] Compared to conventional assays focusing on whole-tissue and terminal readouts, the development of nanosensors (Figure 3) provides an opportunity to dynamically capture information and unveil mechanistic details in vivo that might otherwise be missed in vitro and ex vivo studies.

Tumour hypoxia

Imbalances caused by hypoxia in aerobic and anaerobic respiration exacerbate oxidative stress, which is characterized by the accumulation of reactive oxygen species (ROS)[48], including hydrogen peroxide (H_2O_2), nitric oxide (NO), hydroxyl and superoxide radicals, and oxidatively modified macromolecules such as oxidized thiols, lipids, and carbohydrates[92]. Conventional methods to measure oxygen levels, like the use of pimonidazole and EF5 (a 2-nitroimidazole-based molecule) staining,[93] require cell fixation followed by immunostaining and, thus, preclude continuous measurements in cells or mice. Direct measurement of oxygen levels using extraceullular flux technology (e.g. oxygen consumption rate) can be adapted to certain model organisms (such as the *C. Elegans* or the zebrafish models),[94] but the extracellular assay-based analysis using culture medium lacks precise spatiotemporal resolution in an organ or tissue level. Additionally, hypoxia assays often utilize the reductive cleavage of small molecules under hypoxic conditions. The irreversibility of these assays prevents dynamic monitoring of oxygen levels and may provide misleading information if cleaved nanoprobes translocate to the normoxic region. Several nanosensors technologies were developed to address these challenges (Fig. 2a).

Sensors based on single-walled carbon nanotubes (SWCNT) **[G]** can continuously measure ROS in live cells and in vivo. SWCNTs are photostable and fluoresce in the second near-infrared (NIR) region (1000–1700 nm; NIR-II), where the scattering and absorption of light through tissues and autofluorescence are minimal.[95–97] When in proximity to ROS, the fluorescence intensity of SWCNT sensors is attenuated through a reversible Fermi level shift in the electronic band structure of SWCNT, resulting in bleaching of the absorption transition and concomitant fluorescence quenching[98] (Figure 3a, top). Wrapping SWCNTs with specific moieties can confer sensitivity towards specific ROS species. For example, SWCNT wrapping with a single-stranded-DNA (ssDNA) with the sequence $(GT)_{15}$ confers sensitivity to H_2O_2, singlet oxygen, or hydroxyl radicals.[99] SWCNTs wrapped by an

$(AT)_{15}$ ssDNA or by dextran exhibit reversible fluorescence intensity reduction caused by electron transfer from SWCNT to NO.[100,101] SWCNT-based ROS sensors can trace a broad ROS concentration range (0.07–60 μM for NO and 0.15–0.9 mM for H_2O_2). These nanosensors were successfully used to monitor H_2O_2signalling downstream of EGFR activation in epidermal carcinoma cells[102] and singlet oxygen produced during enzymatic suicide inactivation **[G]**.[103]

In addition, dye-conjugated lanthanide nanoparticles have been developed for the detection of ROS (Figure 3a, middle). The oxidation state of lanthanide-doped fluorophores can be modulated by ROS, resulting in variations in fluorescence intensity and/or fluorescence lifetime. For instance, nanoparticles covered with neodymium ions (Nd^{3+}-doped nanoparticles) that are non-covalently conjugated with the NIR dye MY-1057 exhibit Förster resonance energy transfer (FRET) when in proximity to $ONOO^-$.[104] Peroxynitrite degrades the FRET acceptor MY-1057, recovering the fluorescence lifetime and intensity of the FRET donor Nd^{3+}. Such nanosensors can be useful for deep tissue measurements, as NIR emission lifetime is independent of the depth of tissue penetration. However, ROS-induced oxidation of the NIR dye is irreversible, similar to conventional hypoxia assay. To dynamically monitor ROS, nanosensors carrying reversibly ROS-reactive fluorophores may be used.[105]

Finally, polymeric nanoparticles consisting of oxygen-sensitive platinum(II) porphyrin and the oxygenin-sensitive conjugated polymer polyfluorene were developed to reversibly image hypoxic environments in vivo (Figure 3a, bottom).[106] These nanosensors used ratiometric intensity change to quantify oxygen levels. Specifically, the oxygen-insensitive fluorescence peak was used as an internal reference. The presence of oxygen caused a decrease in the phosphorescence at ~660nm due to energy transfer from the triplet excited state of platinum(II) porphyrin and the triplet oxygen state. The intensity ratio between the peaks at the fluorescence of polyfluorene moieties (420–460nm) and phosphorescence from platinum(II) porphyrin (630–680 nm) linearly correlated with the O_2 concentration, enabling spatiotemporal mapping of resolved oxygen levels in live cells or *in vivo*.

Tumour hyperacidity

The extracellular pH in the TME can vary between 5.8–7.4. This pH variability depends on tumour-intrinsic factors, like aerobic and anaerobic respiration, hypoxia, angiogenesis, perfusion, CO_2 hydration, and proton excretion. Given their dynamic and transient regulation, acidity gradients within intracellular compartments, such as lysosomes of tumour cells, as well as within the TME are not fully understood. Conventional techniques used to detect intracellular pH are unsuitable for temporal tracking of pH and in vivo use. Common acidity probes, as, for example, fluorescent stains, exhibit a time-dependent alkalizing effect on lysosomes[107] and are susceptible to photobleaching upon prolonged excitation.

To directly assess the dysregulated pH in tumours, several optical nanosensors have been developed (Fig. 2a), including tunable pH-sensitive amphiphilic polymers and nanoparticles.[108,109] Polymers comprised of ionizable tertiary amine and poly(ethylene oxide) segments can form pH-activatable micellar nanoparticles (Figure 3b, top). At high pH, the neutralized amine segments self-assemble into micelles due to their increasing

hydrophobicity, and micelle formation results in fluorescence quenching through FRET. At lower pH, micelles disassemble due to protonation at the amines, and the fluorophores brightly fluoresce. The pKa values of ammonium groups and the hydrophobicity of the amine segments can be adjusted to ensure transitions at different pH values. The pH nanoprobe design showed fast (<5ms) and sensitive response (<0.25pH unit). The systematic design of polymers enabled the dynamic range of the nanosensors to cover the entire physiologic pH range (4–7.4) in the visible and NIR regions (400–820 nm). Such nanosensors have been applied in studies with lung and clear cell renal carcinoma cell lines. Nanosensor activation occurred inside the late endosomes and lysosomes and enabled intracellular pH monitoring modulated by a V-ATPase inhibitor.[108]

FRET-based nanosensors composed of the ratiometric pH-sensitive dye ANNA (N-carboxyhexyl derivative of 3-amino-1,2,4-triazole fused 1,8-naphthalimide) and biocompatible metal oxide nanoparticles (Fe_3O_4) were constructed to spatiotemporally map microenvironmental pH in vivo.[110,111] For instance, ANNA was linked with nanoparticles with a peptide substrate of matrix metalloprotease 9 (MMP-9), a frequently detected protease in tumour ECM. FRET between ANNA and substrate-linked nanoparticles quenches the fluorescence, however, MMP-9-mediated peptide–substrate cleavage activates ANNA fluorescence allowing pH measurements specifically within the tumour ECM. Imaging studies using such nanoparticles in a mouse model of human gastric cancer revealed that the tumour extracellular pH is spatially heterogeneous, ranging from 6.6–7.6.[111]

pH-activatable fluorescent nanosensors were developed to monitor metabolic acidosis in solid cancers and are under clinical trials for fluorescence-guided surgery.[112–114] Such nanosensors have a sharp response at pH 6–7 and exploit pH differences between healthy and diseased cells as a biomarker. For instance, pH-low insertion peptides (pHLIPs) exploit the folding and insertion of pH-sensitive peptides across the cell membrane.[114,115] When a pHLIP encounters acidic diseased tissue, the protonatable residues of the peptide become neutral at the surface of the cellular membrane. The protonation leads to an increase in the hydrophobicity of the peptide, triggering pHLIP to partition into the hydrophobic bilayer, resulting in the formation of a stable transmembrane helix. pHLIPs can be conjugated to dyes, such as Cy5 for fluorescence imaging[116] or the IR dye QC1 for optoacoustic imaging[16], and can be radiolabeled for PET imaging[117] to mark the periphery of the tumour (Figure 3b, middle). While acidity-responsive imaging holds great potential for sensitive and specific tumour imaging and reliable imaging-guided tumour resection, the narrow dynamic range of pH-activatable fluorescent nanosensors may limit the degree of spatially mapping the hyperacidity in the TME.

Lastly, plasmonic nanoparticles **[G]** functionalized with pH-sensitive reporter molecules (such as 4-mercaptopyridine and 4-mercaptobenzoic acid) were designed for continuously measuring local pH in live cells via surface-enhanced Raman spectroscopy **[G]** (SERS).[118–121] The Raman probes exhibited quantitative pH-dependent intensity changes in SERS spectra by the protonation state of the reporter molecule. SERS-based pH nanosensors do not photobleach, can be minimally invasive, and have flexible excitation wavelengths. A nanopipette **[G]** functionalized with such plasmonic nanosensors can measure local intracellular pH (Figure 3b, bottom).[120] Raman hyperspectral imaging enables spatially

resolved endolysosomal pH imaging in cells.[118,119] Porous silicon nanoneedle arrays have been used to “nanoinject” pH-sensitive fluorescent dyes to spatially map pH distribution in live OE33 esophageal adenocarcinoma cells.[122]

Tumour metabolism

Stromal, immune, and cancer cells constantly compete for limited nutrients in the TME, and metabolic adaptation reorganizes the nutrient uptake and utilization to favor tumour cell growth.[123,124] While mRNA or protein expression can change at a time scale of hours to days, the level and type of metabolites can change in the target tissue within minutes or seconds.[125] Therefore, robust approaches to investigate key metabolites in the TME in real-time to find potential cancer vulnerabilities are needed (Fig. 2a–c).

Glucose metabolism—Tumour cells rely on glucose to grow and proliferate, and activation of glycolytic pathways in tumour cells causes a shift in the metabolic profile of the TME.[4,123] Additionally, T cells primarily use glucose to sustain their immune surveillance functions in the TME.[4] Leveraging advancements in glucose detection for other diseases, like diabetes, have led to clinical studies monitoring hyperglycemia during chemotherapy (NCT04473378).[126] Glucose oxidase-functionalized nanopipettes have been developed to extend these investigations to the single cell level (Figure 3c, top).[127] The nanopipettes detect the oxidation of β-D-glucose to D-gluconolactone and H_2O_2, measured as a change in electrical impedance. The electrochemical nanoprobe can capture the spatiotemporally resolved glucose levels in cancer cells. Alternatively, a hollow fiber sensor capable of liquid exchange can monitor glucose consumption rate in real-time.[128] Nanopipettes have also been employed as a nanobiopsy platform to sample a small amount of liquid in live cells. Nanopipettes can be inserted into a single cell and collect cytoplasmic materials for post-biopsy analyses for single-cell and spatial genomics, transcriptomics, proteomics, and metabolomics.[129,130]

Tumour cells under hypoxic conditions preferably replenish ATP using glycolysis and secrete lactate, leading to an increase in concentrations of lactate in the TME by up to ten times as compared to healthy tissue regions.[131] Hence, rapid lactate production and secretion by cancer cells is a hallmark characteristic of the TME. Secreted lactate can be utilized non-cell autonomously as an alternative energy source by oxygenated tumour cells[132], or it can disrupt the differentiation of immune cells leading to disabled functions of T- and NK cells. This phenomenon enables cancer cells to evade immunosurveillance.[133]

Commercially available lactate assays are incompatible with continuous monitoring of lactate in live cells and in vivo due to their irreversible detection mechanisms relying on coupled reactions with multiple enzymatic, fluorescent or bioluminescent substrates.[134] To address this challenge, novel optical and electrochemical nanobiosensors that detect secreted lactate were developed.[135,136] The selectivity of the nanosensors was achieved by covalent immobilization of lactate dehydrogenase (LDH). LDH catalyzes the conversion of lactate into pyruvate while reducing the cofactor NAD^+ to NADH. LDH-immobilized optical nanosensors have been employed to measure local lactate levels in live cells by detecting the fluorescence of the enzymatic product, NADH (excitation at 360nm, emission at 460nm).[135]

As the concentration of the generated NADH is proportional to the levels of lactate, a change in NADH fluorescence intensity can reflect changes in concentrations of lactate. LDH-immobilized nanosensors have been used to quantify the extracellular lactate levels in HeLa cells, in MCF7 breast cancer cells, and in human fetal osteoblasts, indicating that via the Warburg effect, cancer cells produce higher lactate levels than normal cells (0.3–0.6mM vs. 0.2mM).[135] Additionally, LDH and gold nanoparticle-embedded electrodes have been developed for the electrochemical detection of lactate. Gold nanoparticles on the electrode catalyze the oxidation of NADH to generate current through an electrocatalytic reaction, which is proportional to NADH and lactate concentrations. Electrochemical sensing with nanowire electrodes enables fast response times and high sensitivity. However, this sensor technology has not yet been employed to measure lactate levels in the TME.[136]

Amino acid metabolism—Amino acid concentrations can differ from the tumour periphery to the tumour core, and tumour cells compete with T cells for amino acid uptake.[4] While both tumour cells and T cells heavily rely on glutamine catabolism, tumor cells can use local cystines to reduce glutamine dependency, and T cells can harness arginines to activate T-cell function and differentiation. Such metabolic adaptation for amino acids can be therapeutically targeted. Thus, there is a need to understand the dynamics and availability of amino acids across the TME. Currently, complete nutrient analysis is performed by mass spectrometry (MS)-based metabolomics of cells, which can only offer an endpoint analysis. Few amino acid nanosensors have been developed due to challenges in differentiating structurally similar small molecules. Nitrogen and sulfur-doped fluorescent carbon dots were developed for dual-sensing of ferric ions and L-cystine (L-Cys) in live Hep G2 cells and in vivo. The carbon dots formed a complex with ferric ions, quenching their red fluorescence (centered at ~600 nm). The addition of L-Cys recovered the carbon dot fluorescence by forming stronger complexation between L-Cys and ferric ions. In addition, covalent functionalization of the nanopipette tip with the DNAzyme **[G]** selectively recognizes L-histidine (L-His), enabling electrochemical sensing of cytosolic amino acids in live cells[137]. Self-cleavage of the DNAzyme by L-His changes the electrical current of the nanopipette. The nanopipette measured intracellular L-His by targeting specific subcellular regions of individual cells and time-dependent quantification of L-His under carnosine and hydrocortisone treatments. Further investigations on application of these sensors to tumour cells and in vivo tumour models are warranted.

Lipid metabolism—Lipid metabolism is substantially altered in cancer cells. Increased de novo lipogenesis and/or uptake of lipids contribute to rapid tumour growth.[138,139] Furthermore, increasing evidence shows that cancer stem cells, which have been implicated in therapy resistance and cancer recurrence, rely on lipid metabolism to maintain their stemness and proliferative capacity.[140] Lipid accumulation within the endolysosomal lumen is also closely related to nonalcoholic steatohepatitis,[141] a strong risk factor for liver cancer.[142] Conventionally, stains such as oil red O are used to detect the general accumulation of lipids within cells and tissues.[143] A number of nanosensors have been developed to study lipid metabolism in cells and *in vivo*. Fluorophore-conjugated and intrinsically fluorescent lipid analogues are used to analyze lipid trafficking, as demonstrated by the tracking of uptake and incorporation of lipids into the cell membrane in A172

glioblastoma cells.[144] Lipid dynamics in live cells can be tracked using fluorescent proteins fused with lipid-binding domains[145] or polarity-sensitive dye-conjugated phospholipid-binding motif of gelsolin (or its short peptide)[146]. SWCNT-based nanosensors that localize specifically to the endolysosomal lumen and report lipid contents in live cells were developed.[107,147] The hydrophobic interactions between ss$(GT)_6$-wrapped or ss$CT_2C_3T_2C$-wrapped SWCNT surface and biological lipids decrease the local solvent dielectric, leading to a solvatochromic shift **[G]** in SWCNT fluorescence. The nanosensors enabled the mapping of heterogeneity in lipid levels across lysosomal compartments in bone-marrow-derived monocytes[107] and measured the dynamics of lysosomal lipid flux in liver macrophages non-invasively in vivo via near-infrared imaging.[147]

Oncometabolites—Oncometabolites are a class of unique metabolites specifically present in tumours.[148,149] They can be found in tumour cells within the TME, accumulating in abnormal concentrations[150] as a result of mutations in genes encoding metabolic enzymes. Sensors based on fluorescent indicator proteins were developed for real-time monitoring of metabolite levels and have successfully screened several small molecules in subcompartments in living cells.[151,152] These nanosensors typically consist of a ligand-sensing domain, allosterically coupled to a pair of fluorescent protein variants capable of FRET. Metabolite binding induces conformational changes that alter the nanosensor FRET efficiencies, allowing for estimation of metabolite levels with micromolar affinity. Alternatively, synthetic molecular recognition **[G]** can be used to replace the protein moieties of metabolite-specific nanosensors.[153] In synthetic molecular recognition-based nanosensors, sensing relies on physisorption and/or close interactions between polymer-wrapped SWCNTs (sensing agent) and target analytes, although no molecularly specific binding site is present in the SWCNT (Figure 3c, bottom). For example, an SWCNT-based optical nanosensor was developed for detecting D-2-hydroxyglutarate (D2HG), an oncometabolite in cancer cells with mutated isocitrate dehydrogenase.[154] Screening of a library of ssDNA-wrapped SWCNTs identified an ssDNA sequence of $(ATTT)_7$ that modulates SWCNT fluorescence intensity within pathological levels of D2HG found in gliomas, acute myeloid leukemia, and breast cancer.[155] The fluorescence response of $(ATTT)_7$-wrapped SWCNT could discriminate D2HG from other related metabolites, including its enantiomer. Such SWCNT nanosensor could be used to detect oncometabolites with subcellular spatial and high temporal resolution, though the compatibility of the nanosensor in cellular environments has not been optimized yet.[156]

Autophagy

In addition to measuring specific metabolites at the TME using nanosensors, metabolic insights can be gained through the monitoring of cellular processes that are triggered under nutrient deprivation. Tumor cells activate autophagic pathways both intrinsically and in surrounding stromal cells, including CAFs, to recycle cellular components and thereby sustain their survival and metabolic needs.[157] However, prolonged activation of the autophagic pathways can induce autophagy-associated cell death.[158] Hence, autophagy sensors for high spatiotemporal resolution at TME could facilitate the understanding of autophagy in cancers (Fig. 2b). As lysosomes are hyperacidified in cells undergoing autophagy, pH nanosensors can be used to map autophagy flux in live cells.[119,159]

Plasmonic nanosensors were developed to track autophagy process via real-time detection of intracellular ROS in the breast cancer cell line MCF7.[160] As some of the pH and ROS nanosensors described in the previous section have already been applied in xenograft models,[110,111] they can be potentially engineered to specifically traffic into the lysosomes for measuring autophagy.

Immunoediting and inflammation

During cancer immunoediting, the immune system constrains the expansion of immunogenic cancer cell clones, leading to the selection and escape of less immunogenic clones. Cancer cell clones that escape immune surveillance are believed to contribute to tumour progression and advancement.[74] Thus, monitoring immune responses can help elucidate the relationship between tumour cells and the immune system and facilitate the development of strategies to immunologically target tumours or overcome immunotherapy resistance.[4,5,8,74] Immunoassays and flow cytometry are widely used to investigate immune responses in the TME. However, these techniques are incompatible with longitudinal tracking of changes in the TME due to their inherent nature as endpoint experiments. Therefore, obtaining spatial resolution to investigate questions pertaining to T cell response in the TME still presents major challenges.[125] Sensor technologies that can detect immune cells, immunocytokines, and ROS were developed (Fig. 2f,g).

Multiple nanoscale imaging agents can monitor the expression of immune checkpoint receptors **[G]**, including programmed cell death 1 (PD-1), programmed cell death ligand 1 (PD-L1), cytotoxic T lymphocyte-associated antigen 4 (CTLA-4), and lymphocyte activation gene 3 (LAG-3), and detect immune cells in the TME using positron emission tomography (PET), computed tomography (CT), and magnetic resonance imaging (MRI) as reviewed elsewhere[161] (Figure 3d, left). Such agents are often constructed through the conjugation of radiolabels or paramagnetic nanoparticles to ligands that specifically bind to immune checkpoint biomarkers and enable high-resolution spatial imaging of these biomarkers within the TME.

Electrochemical aptamer-based biosensors enable real-time molecular measurements in vivo for pharmacodynamic studies[162,163] and biomarker monitoring in non-cancer disease models (Figure 3d, right).[164] These sensors employ electrochemistry to interrogate a binding-induced conformational change in an electrode-bound, redox reporter-modified aptamer. The recognition of small-molecule targets by receptors induces conformational changes, affecting the rate of electron transfer and thus changing the intensity of the electrochemical signal. This sensor platform can be applied to cancer-specific pharmacodynamic studies by incorporating aptamers specific to immune checkpoint receptors, such as PD-L1, and immune cell receptors, such as CD16[165].

Lastly, ROS can be used as a marker for inflammation. During the innate immune response, phagocytes, like neutrophils and macrophages, spontaneously increase ROS production to clear damaged cells via oxidative stress.[48] During adaptive immune responses, T-cell receptor activation triggers the generation of ROS inside T cells to support T-cell activation and cytokine secretion[48]. Polymeric nanoparticles with superoxide anion ($O_2^{\bullet -}$)-activatable

chemiluminescence reporters have been exploited for in vivo imaging of T-cell activation in the TME.[166]

Proteolytic activity

Extracellular proteases—The proteolytic activity of the TME has been heavily explored and has been therapeutically targeted in various cancers.[167,168] Hundreds of TME-associated proteases have been implicated in cancer cell proliferation, invasion and metastasis, and in angiogenesis.[169] For example, cathepsin B, a tumour-enriched protease, has optimal enzymatic activities in an acidic environment and is known to remodel ECM.[170] Protease-responsive optical sensors were developed[110,171–174] to spatially map the TME proteolytic landscape (Fig. 2e). As also mentioned under the subsection on tumour hyperacidity, a FRET-based nanosensor was developed to simultaneously detect protease activity and pH in the TME. The nanosensor was constructed by linking a Fe_3O_4 nanoparticle with a pH-sensitive dye (ANNA) and the NIR dye Cy 5.5 via an enzymatically cleavable peptide linker (Figure 3e).[110] Upon reaching the tumour, the peptide linker connecting ANNA to the nanoparticle is cleaved by MMP-9, and this cleavage results in the activation of the pH-sensing fluorophore. MMP-9 activity was quantified by comparing the activated emission of ANNA against the constant fluorescence of Cy5.5. Imaging studies using a mouse model of human colon cancer revealed that the overexpression of MMP-9 and abnormal microenvironmental pH are spatially heterogeneous and synergistically promote tumour invasion.[110]

Intracellular proteases and cell death—Intracellular protease activities are associated with different types of programmed cell death. For instance, caspase-3 activation is a hallmark of apoptosis.[175] As many cancers develop anti-apoptotic mechanisms to evade cell death, a variety of nanosensors were devised to monitor the induction of apoptosis in live cells. Graphene oxide- and gold nanoparticle-based nanosensors were developed for real-time, live cell imaging of apoptosis markers via surface functionalization with Cy5-labelled cytochrome c aptamers and fluorescein-labeled caspase-3 recognition peptides (Fig. 2c).[176,177] The Cy5 and fluorescein signals are quantitatively turned on based on the activities of cytochrome c and caspase-3, respectively.

Nanosensors for in vivo application—The development of reversible, robust, and biocompatible biosensors enable dynamic monitoring of biological processes/analytes in the TME, facilitating in vivo cancer studies. Current methods, for example, for determining the levels and types of lymphocytes and cytokines in whole blood and tumour tissue biopsies, are often invasive and ineffective in reflecting the dynamic processes occurring in tumour ecosystems. Nanoreporters have the potential to longitudinally and non-invasively assess biological processes, as well as detect key analytes in vivo. Several nanoengineered sensing materials and measurement techniques discussed in previous sections (Table 1) have the potential to detect analytes in live animals, but only a few biosensors have demonstrated efficacy in preclinical animal studies or have been approved for implantation in humans.

Targeted delivery and uptake of nanosensors remain largely unexplored in in vivo cancer models. Effective delivery strategies to control biodistribution will facilitate the in vivo

application of such sensors. Injecting nanoparticles directly into the tumour can sometimes cause physical disruption. Therefore, less invasive TME targeting approaches should be investigated. Nanoparticles can “passively” accumulate within the TME in mouse tumour models via the enhanced permeability and retention **[G]** (EPR) effect (although this mechanism is a subject of some debate[178]). Surface coating of sensors with antifouling and/or stabilizing agents may be necessary. Selective accumulation and retention of nanosensors within the TME may be modulated as a function of the physicochemical properties of nanoparticles, such as size, shape, and surface chemistry.[179] Localization of nanosensors to specific TME compartments can be achieved via surface functionalization with ligands that bind specific ECM components or cell surface targets. For instance, encapsulation of nanosensors with peptides that bind a cell surface receptor facilitates the targeting of a nanosensor to angiogenic vasculature within solid tumours.[180]

Biocompatibility concerns may arise from phototoxicity in long-term and/or deep-tissue imaging. Sensor mechanisms may involve transmission via radionuclides, magnetic resonance, optical, or other mechanisms. Optical sensors that can be excited and fluoresce at the NIR region, such as SWCNTs, can improve upon the use of visible wavelengths. Visible light overlaps with strong tissue scattering, absorption, and autofluorescence, preventing deep tissue imaging and causing phototoxic damage to cells in the tissue. The development of highly phosphorescent or fluorescent nanosensors in the NIR-I (650–1000 nm) or NIR-II windows (1000–1700 nm) can reduce photocytotoxicity and improve light penetration substantially.

Finally, incorporating nanosensors into implantable or wearable devices could facilitate long-term monitoring and improve their translational potential. Nanosensors can be encapsulated into microfibrous textiles to fabricate wearable optical textiles to monitor local oxidative stress[181] or be incorporated into semi-permeable implantable membranes or nanoneedle arrays to monitor TME biomarkers.[122,182,183] Such platforms can be extended as diagnostics and prognostic tools to detect abnormal conditions earlier. Nanosensors and biosensors may enable minimally invasive, real-time, in vivo imaging without missing important biological information. Moreover, they could facilitate longitudinal tracking of tumours, uncovering spatially-resolved tumour heterogeneity in vivo, or measuring temporal responses to therapeutic treatment, and other metrics.

Outstanding Questions, Challenges, and Opportunities

A fundamental understanding of the complex interactions within cancer ecosystems is essential to establish a systems view of cancer biology, find new therapeutic vulnerabilities, enable early diagnoses, and improve clinical outcomes. To address complex problems in cancer biology, new approaches are warranted that combine the expertise of engineers, biologists, and clinicians. Engineering-based interdisciplinary research tools hold promise in overcoming limitations associated with conventional tumour models, assays, and research designs by better reflecting and monitoring heterogeneity in tumour ecosystems. In a systemic or cellular perspective, advanced tumour models can control intercellular densities, structure, nutrient gradients, oxygen gradients, chemokine gradients, and physical forces, and introduce multiple cell types and perfused vasculature. In a cellular or molecular

perspective, optical, radio-emitting, and electrical nanoscale technologies have been developed to monitor biomarkers in tumour cells and in vivo. Engineering approaches, thus, offer increasingly powerful capabilities, including the modeling and monitoring of the TME-associated signaling pathways and the detection of biomarkers with spatiotemporal resolution. However, many promising nanosensor technologies have not yet been deployed in cancer research. Thus, there is potential for the synergistic application of these technologies in tumour models. Additionally, combining genetic engineering or synthetic biology approaches with nanotechnologies can help expand the tools available to understand the *in vivo* dynamics of protein expression and/or genetic alterations (Box 2).

For many important problems and questions in cancer biology, new technologies may be required to adequately address them. Foremost, there is an unmet need for improved cancer models that recapitulate in vivo 3D environments. Many models exist, but most have not been validated rigorously in prospective co-clinical trials. Specifically, there is a need for models that better capture the plasticity of cancer systems, especially integrating multiple tissue types and tumour sites, including primary tumours, sentinel lymph nodes **[G]**, and metastatic sites. Also, models that can be maintained for longer time points to better model evolutionary dynamics of tumours as they progress, and respond to various stresses, are needed. Models that connect various engineered tissue types such as kidney, gut, liver, and tumour in specific tissues could be valuable for drug pharmacokinetics and pharmacodynamics studies. Technologies that report how RNA, protein, and/or metabolite levels change within or around cells in vivo in response to various stimuli and over time would be valuable. In addition, extractable or ex vivo trackable nanosensors that can report on tissue-specific interstitial fluid metabolite concentrations in vivo would address unmet needs in cancer metabolism. Currently, in vivo detection of specific cytokines, metabolites, or other chemicals that are in contact with cells, and of their changes over time, in response to various stimuli, remain elusive.

Apart from their use as tools in basic research or drug discovery, an increasing number of investigations have demonstrated the translational potential of micro- and nanotechnologies for disease detection, risk assessment, progress monitoring, prediction of responses to therapy, and personalized treatment (Table 2). Micro- and nanoengineered tumour models mimicking dynamic and complex physiological characteristics of the TME can be used for high-throughput screening assays to identify personalized treatment options or robust and reproducible prediction of clinical response. For example, a microfluidic preclinical platform was developed for multiplexed cancer drug testing in slice cultures from human glioma xenografts and patient tumor biopsies.[184] In another study, microfluidic-based cell invasion assays were used for the patient-specific prediction of progression-free survival and recurrence time in patients with glioblastoma.[185]

Nanosensor technologies provide insights into efficacy, resistance, and toxicity for therapeutic interventions. Rather than relying on survival studies and histology-based methods, longitudinal and non-invasive monitoring with nanosensors can be a substitute for large in vivo studies and decrease the delay to obtain readouts for preclinical and clinical endpoints in drug development research for the optimization of targeted therapies. These technologies can be useful to study and optimize in vivo pharmacodynamics,

pharmacokinetics, intratumoural penetration, and cargo delivery mechanisms that can be significantly different from those observed in experiments performed in vitro.

Finally, the development of nanotechnology tools that enrich and isolate cancer-derived bioanalytes from patient biofluids would enable the development of noninvasive tests for cancer screening, diagnosis, or monitoring[186] and facilitate multi-omics-based biomarker discovery, the investigation of molecular mechanisms, and the design of personalized therapies.[15]

Many outstanding questions and problems remain unaddressed to improve clinical outcomes, presenting translational opportunities for (nano)engineers. For instance, within the field of precision prevention, increasing evidence suggests that normal epithelia harbour mutated cells that may eventually turn malignant. The development of new detection technologies that continuously monitor biomarkers, or simple liquid biopsy screening methods[183,186], potentially enables low-volume and/or early-stage cancer detection. These methods could be deployed in high-risk individuals with cancer predisposition genetic syndromes (such as familial adenomatous polyposis) or chronic inflammatory diseases (such as inflammatory bowel disease). In cancer treatment, highly sensitive and specific imaging technologies that can identify single or small clusters of malignant cells[116,187,188] could be developed to improve the identification of residual cancer cells intraoperatively while minimizing the need to remove large amounts of normal tissue to achieve good resection margins. Bioengineering approaches and nanomaterials that can be administered systemically and retrieved later to longitudinally collect biological material, such as nucleic acids, protein, metabolites, or even cells from tumours, would help monitor drug delivery and efficacy. Tissue embeddable and retrievable, or circulating, sensors of drug uptake, metabolism, and perhaps also activity, would be beneficial.

Acknowledgements

This work was supported in part by the NIH (R01-CA215719, R01-NS116353, R01-NS122987, R01-DK129299 and the Cancer Center Support Grant, P30-CA008748), the National Science Foundation CAREER Award (1752506), the American Cancer Society Research Scholar Grant (GC230452), the Ara Parseghian Foundation, the Honorable Tina Brozman Foundation for Ovarian Cancer Research, the Ovarian Cancer Research Alliance (CRDGAI-2023-3-1003), the Pershing Square Sohn Cancer Research Alliance, the Expect Miracles Foundation – Financial Services Against Cancer, Emerson Collective, the Experimental Therapeutics Center, Mr. William H. Goodwin and Mrs. Alice Goodwin and the Commonwealth Foundation for Cancer Research, Burroughs Wellcome Funds, AACR, Stand Up to Cancer. M.K. was supported by the NIH (K99-EB033580) and the Marie-Josée Kravis Women in Science Endeavor Postdoctoral Fellowship. M.P. was supported by an NIH grant (5T32CA062948). S.R. was supported by the MERIT Mandel Fellowship, Memorial Sloan Kettering Cancer Center.

Competing interests

D.A.H. is a co-founder and officer with equity interest in Lime Therapeutics, Inc., and co-founder with equity interest in Selectin Therapeutics Inc., and Resident Diagnostics, Inc., and a member of the scientific advisory board of Concarlo Therapeutics, Inc., Nanorobotics Inc., and Mediphage Bioceuticals, Inc. T.T. has research support from ONO Pharma USA., Inc. (unrelated to this work) and is a member of the scientific advisory board of Lime Therapeutics, Inc. with equity interest. M.K., M.P., C.C., S.B.R., and K.G. declare no competing interests.

Glossary

Hypoxia

A subnormal concentration of oxygen. In cancer tissue, hypoxia is often the result of abnormal vasculature

Immunoediting
Describes the complex relationship between a developing tumour under constant pressure from the host immune system. Cancer immunoediting consists of three phases: elimination (that is, cancer immunosurveillance), equilibrium and escape. The immune system not only protects the host against development of primary cancers but also sculpts tumour immunogenicity

Multicellular spheroids
Multicellular spheroids are either self-assembling or are forced to grow as 3D spherical cell clusters. They can be established from a single cell type or can be multicellular mixtures of tumour, stromal, and immune cells. These aggregates can mimic tumour cell behavior more effectively because they harbor a gradient of cells that are surface-exposed and cells that are deeply buried thereby also estabishing a gradient of nutrient and oxygen availability

Organoids
Organoids are tissue-like 3D cultures originating from human stem cells, organ-specific progenitor cells, or dissociated tumour tissues, grown in a reconstituted extracellular matrix. Organoids mimic primary tissues by retaining some aspects of tissue architecture and function. Tumour-derived organoids retain the diversity and fidelity of mutational landscapes, and, when transplanted into mice, reconstitute many of the histopathological features of their tumours of origin

Genetic drift
Changes in the frequency of a genetic variant in a population owing to chance alone

Bottleneck effects
A population bottleneck is an event that drastically reduces the size of a population. Bottlenecks produce a decrease in the gene pool of the population because many alleles, or gene variants, that were present in the original population are lost. Due to the loss of genetic variation, the new population can become genetically distinct from the original population

Mouse tumour xenograft models
Hetero-transplantation of human tumour cells into immunodeficient mice, in either the orthotopic (same organ) site or ectopic (foreign) site. Mice are typically athymic nu/nu T cell deficient or severe combined immunodeficient (SCID), lacking B cell and T cell functions

Electrospun nanofibers
Fibers with diameters in the nanometer range created using electrospinning. Electrospining relies on the electrostatic repulsion between surface charges to continiously draw nanofibers from a viscoelastic fluid

Nanoprinted scaffolds

3D-scaffolds with nanometer scale features that mimic interstitial tissue or extracellular matrix. They are used either as cell migration or tumor formation platforms

Microfluidic systems
These small ‘plumbing’ systems deal with the accurate control and manipulation of fluids that are confined to micron-sized environments. This enables the supply of nutrients, oxygen and the flow of media to be precisely controlled

Microcontact printing
Microcontact printing is a method of transferring patterns of various materials such as polymers, proteins, nanoparticles, etc., onto another surface. Typically a polydimethylsiloxane (PDMS) stamp is dipped in a solution of a material that has to be patterned and is brought into contact with the surface

Chemokines
A family of inducible chemoattractant cytokines that regulate the chemotaxis of tumour cells and other cell types. Chemokines also affect processes such as proliferation, migration and invasion

Mechanotransduction
Mechanisms by which cells convert mechanical stimulus into biochemical signals

Gefitinib
The first quinazoline-based reversible small-molecule EGFR tyrosine kinase inhibitor

Sacrificial bioink
A biomaterial used as ink in 3D printing of biomimetic structures, that has gentle and reversible crosslinking properties and can be easily removed (or “sacrificed”) without harming the involved cells and structures

Nanolithography
Set of top-down fabrication techniques that allow patterning materials and building devices with nanoscale resolution

Vascular lumen
The inside space of a vessel, composed of a cord of endothelial cells

Self-assembled microvessels
Spontaneously created in vitro vascular networks driven by inherent cellular interactions between endothelial cells and stromal cells to undergo morphogenesis

Cytokines
Small, secreted proteins produced by immune cells that are used in cellular communication

Single-walled carbon nanotubes
sp^2-hybridized carbon-based hollow cylindrical nanostructures that exhibit unique electronic and optical properties for intracellular and in vivo imaging and sensing

Enzymatic suicide inactivation
Irreversible or permanent inhibition of an enzymatic activity

Plasmonic nanoparticles
Metallic nanoparticles whose electron density can couple with certain wavelengths of light. Plasmonic nanoparticles exhibit interesting scattering, absorbance, and coupling properties based on their structures, geometries, and relative positions

Surface-enhanced Raman spectroscopy
Highly sensitive technique that enhances the Raman scattering of molecules supported by nanostructured materials

Nanopipette
A nanoscale pipette that locally collects analytes for mass spectrometry, electrochemical, and optical analysis

Synthetic molecular recognition
Recognition of target analytes conferred by synthetic polymers that create a selective molecular recognition site on a nanoparticle for the molecule of interest, leading to sensitive and selective optical response

Dnazyme
Single-stranded DNA oligonucleotides with high catalytic activities toward specific substrates

Solvatochromic shift
Phenomenon in which emission wavelength of a fluorophore changes in response to the dielectric constant of its environment

Immune checkpoint receptors
Cell-surface molecules that are expressed by T cells and the normal function of which is to maintain self-tolerance and regulate the magnitude and duration of immune responses. Checkpoint receptors, including PD1 and TIM3, can be co-opted by tumours to inhibit antitumour immune responses

Enhanced permeability and retention effect
Compared to healthy tissues, some tumors exhibit increased permeability and renteion for large moelcular weight molecules primarily due to structural abnormality of tumor vasculature

Sentinel lymph node
The first lymph node that connects to a primary tumor site, also it is likely the first lymph node where cancer cells spread

References

1. Wu F et al. Single-cell profiling of tumor heterogeneity and the microenvironment in advanced non-small cell lung cancer. Nat Commun 12, 2540, doi:10.1038/s41467-021-22801-0 (2021). [PubMed: 33953163]

2. Yan Y et al. Understanding heterogeneous tumor microenvironment in metastatic melanoma. PLOS ONE 14, e0216485, doi:10.1371/journal.pone.0216485 (2019). [PubMed: 31166985]
3. Lee Y et al. XYZeq: Spatially resolved single-cell RNA sequencing reveals expression heterogeneity in the tumor microenvironment. Sci Adv 7, eabg4755, doi:10.1126/sciadv.abg4755 (2021).Spatially resolved single-cell RNA sequencing informs how cell type composition and cellular states relate to location within complex pathological tissue.
4. Elia I & Haigis MC Metabolites and the tumour microenvironment: from cellular mechanisms to systemic metabolism. Nat Metab 3, 21–32, doi:10.1038/s42255-020-00317-z (2021). [PubMed: 33398194]
5. Li F & Simon MC Cancer Cells Don't Live Alone: Metabolic Communication within Tumor Microenvironments. Dev Cell 54, 183–195, doi:10.1016/j.devcel.2020.06.018 (2020). [PubMed: 32640203]
6. Lyssiotis CA & Kimmelman AC Metabolic interactions in the tumor microenvironment. Trends Cell Biol 27, 863–875, doi:10.1016/j.tcb.2017.06.003 (2017). [PubMed: 28734735]
7. Belotti D, Pinessi D & Taraboletti G Alternative vascularization mechanisms in tumor resistance to therapy. Cancers (Basel) 13, 1912 (2021). [PubMed: 33921099]
8. Klemm F et al. Interrogation of the Microenvironmental Landscape in Brain Tumors Reveals Disease-Specific Alterations of Immune Cells. Cell 181, 1643–1660.e1617, doi:10.1016/j.cell.2020.05.007 (2020). [PubMed: 32470396]
9. Rothschilds AM & Wittrup KD What, why, where, and when: Bringing timing to immuno-oncology. Trends Immunol 40, 12–21, doi:10.1016/j.it.2018.11.003 (2019). [PubMed: 30545676]
10. Kim SC, Clark IC, Shahi P & Abate ARJA c. Single-cell RT-PCR in microfluidic droplets with integrated chemical lysis. Anal Chem 90, 1273–1279, doi:10.1021/acs.analchem.7b04050 (2018). [PubMed: 29256243]
11. Chen Michelle B et al. Inflamed neutrophils sequestered at entrapped tumor cells via chemotactic confinement promote tumor cell extravasation. Proc Natl Acad Sci U S A 115, 7022–7027, doi:10.1073/pnas.1715932115 (2018). [PubMed: 29915060]
12. Ronaldson-Bouchard K et al. A multi-organ chip with matured tissue niches linked by vascular flow. Nat Biomed Eng 6, 351–371, doi:10.1038/s41551-022-00882-6 (2022). [PubMed: 35478225]
13. Neufeld L et al. Microengineered perfusable 3D-bioprinted glioblastoma model for in vivo mimicry of tumor microenvironment. Sci Adv 7, eabi9119, doi:10.1126/sciadv.abi9119 (2021).
14. Kim M et al. Detection of ovarian cancer via the spectral fingerprinting of quantum-defect-modified carbon nanotubes in serum by machine learning. Nat Biomed Eng 6, 267–275, doi:10.1038/s41551-022-00860-y (2022). [PubMed: 35301449]
15. Gardner L, Kostarelos K, Mallick P, Dive C & Hadjidemetriou M Nano-omics: Nanotechnology-based multidimensional harvesting of the blood-circulating cancerome. Nat Rev Clin Oncol 19, 551–561, doi:10.1038/s41571-022-00645-x (2022). [PubMed: 35739399]
16. Roberts S et al. Acid specific dark quencher QC1 pHLIP for multi-spectral optoacoustic diagnoses of breast cancer. Sci Rep 9, 8550, doi:10.1038/s41598-019-44873-1 (2019). [PubMed: 31189972]
17. Yamada KM & Cukierman E Modeling tissue morphogenesis and cancer in 3D. Cell 130, 601–610, doi:10.1016/j.cell.2007.08.006 (2007). [PubMed: 17719539]
18. Huang L et al. PDX-derived organoids model in vivo drug response and secrete biomarkers. JCI Insight 5, doi:10.1172/jci.insight.135544 (2020).
19. Kim J, Koo B-K & Knoblich JA Human organoids: model systems for human biology and medicine. Nat Rev Mol Cell Biol 21, 571–584, doi:10.1038/s41580-020-0259-3 (2020). [PubMed: 32636524]
20. Dao V, Yuki K, Lo YH, Nakano M & Kuo CJ Immune organoids: From tumor modeling to precision oncology. Trends Cancer 8, 870–880, doi:10.1016/j.trecan.2022.06.001 (2022). [PubMed: 35773148]
21. Bose S, Clevers H & Shen X Promises and challenges of organoid-guided precision medicine. Med (N Y) 2, 1011–1026, doi:10.1016/j.medj.2021.08.005 (2021).
22. Neufeld L et al. Microengineered perfusable 3D-bioprinted glioblastoma model for in vivo mimicry of tumor microenvironment. Sci Adv 7, eabi9119, doi:10.1126/sciadv.abi9119 (2021).

23. Neufeld L, Yeini E, Pozzi S & Satchi-Fainaro R 3D bioprinted cancer models: from basic biology to drug development. Nat Rev Cancer 22, 679–692, doi:10.1038/s41568-022-00514-w (2022). [PubMed: 36280768]
24. Izumchenko E et al. Patient-derived xenografts effectively capture responses to oncology therapy in a heterogeneous cohort of patients with solid tumors. Ann Oncol 28, 2595–2605, doi:10.1093/annonc/mdx416 (2017). [PubMed: 28945830]
25. Yoshida G Applications of patient-derived tumor xenograft models and tumor organoids. J. Hematol Oncol 13, 1–16, doi:10.1186/s13045-019-0829-z (2020). [PubMed: 31900191]
26. Katti A, Diaz BJ, Caragine CM, Sanjana NE & Dow LE CRISPR in cancer biology and therapy. Nat Rev Cancer 22, 259–279, doi:10.1038/s41568-022-00441-w (2022). [PubMed: 35194172]
27. Liu Y et al. Mammalian models of chemically induced primary malignancies exploitable for imaging-based preclinical theragnostic research. Quant Imaging Med Surg 5, 708, doi:10.3978/j.issn.2223-4292.2015.06.01 (2015). [PubMed: 26682141]
28. Chen S, Boda SK, Batra SK, Li X & Xie J Emerging roles of electrospun nanofibers in cancer research. Adv Healthc Mater 7, 1701024, doi:10.1002/adhm.201701024 (2018).
29. Wang Y & Yao Y Nanofiber alignment mediates the pattern of single cell migration. Langmuir 36, 2129–2135, doi:10.1021/acs.langmuir.9b03314 (2020). [PubMed: 32040329]
30. Panagiotakopoulou M et al. A nanoprinted model of interstitial cancer migration reveals a link between cell deformability and proliferation. ACS Nano 10, 6437–6448, doi:10.1021/acsnano.5b07406 (2016). [PubMed: 27268411]
31. Lemma ED et al. Microenvironmental stiffness of 3D polymeric structures to study invasive rates of cancer cells. Adv Healthc Mater 6, 1700888, doi:10.1002/adhm.201700888 (2017).
32. Yang Y, Kulangara K, Sia J, Wang L & Leong KWJ Engineering of a microfluidic cell culture platform embedded with nanoscale features. Lab Chip 11, 1638–1646 (2011). [PubMed: 21442110]
33. Irimia D, Charras G, Agrawal N, Mitchison T & Toner M Polar stimulation and constrained cell migration in microfluidic channels. Lab Chip 7, 1783–1790, doi:10.1039/b710524j (2007). [PubMed: 18030401]
34. Pathak A & Kumar S Independent regulation of tumor cell migration by matrix stiffness and confinement. Proc Natl Acad Sci U S A 109, 10334–10339, doi:10.1073/pnas.1118073109 (2012). [PubMed: 22689955]
35. Lin B, Yin T, Wu YI, Inoue T & Levchenko A Interplay between chemotaxis and contact inhibition of locomotion determines exploratory cell migration. Nat Commun 6, 6619, doi:10.1038/ncomms7619 (2015). [PubMed: 25851023]
36. Wilson K et al. Mechanisms of leading edge protrusion in interstitial migration. Nat Commun 4, 2896, doi:10.1038/ncomms3896 (2013). [PubMed: 24305616]
37. Liu YJ et al. Confinement and low adhesion induce fast amoeboid migration of slow mesenchymal cells. Cell 160, 659–672, doi:10.1016/j.cell.2015.01.007 (2015). [PubMed: 25679760]
38. Maiuri P et al. Actin flows mediate a universal coupling between cell speed and cell persistence. Cell 161, 374–386, doi:10.1016/j.cell.2015.01.056 (2015). [PubMed: 25799384]
39. Lin B et al. Synthetic spatially graded Rac activation drives cell polarization and movement. Proc Natl Acad Sci U S A 109, E3668–3677, doi:10.1073/pnas.1210295109 (2012). [PubMed: 23185021]
40. Fetah KL et al. Cancer modeling-on-a-chip with future artificial intelligence integration. Small 15, 1901985, doi:10.1002/smll.201901985 (2019).
41. Han B, Qu C, Park K, Konieczny SF & Korc M Recapitulation of complex transport and action of drugs at the tumor microenvironment using tumor-microenvironment-on-chip. Cancer Lett 380, 319–329, doi:10.1016/j.canlet.2015.12.003 (2016). [PubMed: 26688098]
42. Wu Q et al. Organ-on-a-chip: Recent breakthroughs and future prospects. Biomed Eng Online 19, 1–19, doi:10.1186/s12938-020-0752-0 (2020). [PubMed: 31915014]
43. Zheng F et al. Organ-on-a-Chip Systems: microengineering to biomimic living systems. Small 12, 2253–2282, doi:10.1002/smll.201503208 (2016). [PubMed: 26901595]

44. Orcheston-Findlay L, Hashemi A, Garrill A & Nock V A microfluidic gradient generator to simulate the oxygen microenvironment in cancer cell culture. Microelectron Eng 195, 107–113, doi:10.1016/j.mee.2018.04.011 (2018).
45. Ma Y-HV, Middleton K, You L & Sun YJM A review of microfluidic approaches for investigating cancer extravasation during metastasis. Microsyst Nanoeng 4, 1–13, doi:10.1038/micronano.2017.104 (2018). [PubMed: 31057891]
46. Chen MB et al. On-chip human microvasculature assay for visualization and quantification of tumor cell extravasation dynamics. Nat Protoc 12, 865–880, doi:10.1038/nprot.2017.018 (2017). [PubMed: 28358393]
47. Rothbauer M, Zirath H & Ertl P Recent advances in microfluidic technologies for cell-to-cell interaction studies. Lab Chip 18, 249–270, doi:10.1039/c7lc00815e (2018). [PubMed: 29143053]
48. Weinberg F, Ramnath N & Nagrath D Reactive oxygen species in the tumor microenvironment: An overview. Cancers (Basel) 11, 1191, doi:10.3390/cancers11081191 (2019). [PubMed: 31426364]
49. Place TL, Domann FE & Case AJ Limitations of oxygen delivery to cells in culture: An underappreciated problem in basic and translational research. Free Radic Biol Med 113, 311–322, doi:10.1016/j.freeradbiomed.2017.10.003 (2017). [PubMed: 29032224]
50. Ando Y et al. Evaluating CAR-T cell therapy in a hypoxic 3D tumor model. Adv Healthc Mater 8, 1900001, doi:10.1002/adhm.201900001 (2019).
51. Aung A, Kumar V, Theprungsirikul J, Davey SK & Varghese S An engineered tumor-on-a-chip device with breast cancer–immune cell interactions for assessing T-cell recruitment. Cancer Res 80, 263–275, doi:10.1158/0008-5472.CAN-19-0342 (2020). [PubMed: 31744818]
52. Pavesi A et al. A 3D microfluidic model for preclinical evaluation of TCR-engineered T cells against solid tumors. JCI insight 2, doi:10.1172/jci.insight.89762 (2017).Three-dimensional modeling approach for systematic analysis of the hypoxic microenviroment.
53. Barmaki S et al. A microfluidic chip architecture enabling a hypoxic microenvironment and nitric oxide delivery in cell culture. Micromachines 11, 979 (2020). [PubMed: 33143339]
54. Shirure VS et al. Quantitative design strategies for fine control of oxygen in microfluidic systems. Lab Chip 20, 3036–3050, doi:10.1039/d0lc00350f (2020). [PubMed: 32716448]
55. Wang X, Liu Z & Pang Y Concentration gradient generation methods based on microfluidic systems. RSC Adv 7, 29966–29984, doi:10.1039/C7RA04494A (2017).
56. Haessler U, Kalinin Y, Swartz MA & Wu M An agarose-based microfluidic platform with a gradient buffer for 3D chemotaxis studies. Biomed Microdevices 11, 827–835, doi:10.1007/s10544-009-9299-3 (2009). [PubMed: 19343497]
57. Allen SG et al. Macrophages enhance migration in inflammatory breast cancer cells via RhoC GTPase signaling. Sci Rep 6, 1–11, doi:10.1038/srep39190 (2016). [PubMed: 28442746]
58. Guo Z et al. M2 macrophages promote NSCLC metastasis by upregulating CRYAB. Cell Death Dis 10, 1–11, doi:10.1038/s41419-019-1618-x (2019).
59. Ren X, Alamri A, Hipolito J, Lin F & Kung SK Applications of microfluidic devices in advancing NK-cell migration studies. Methods Enzymol 631, 357–370, doi:10.1016/bs.mie.2019.05.052 (2020). [PubMed: 31948557]
60. Sai J, Rogers M, Hockemeyer K, Wikswo JP & Richmond A Study of chemotaxis and cell–cell interactions in cancer with microfluidic devices. Methods Enzymol 570, 19–45, doi:10.1016/bs.mie.2015.09.023 (2016). [PubMed: 26921940]
61. Kwapiszewska K, Michalczuk A, Rybka M, Kwapiszewski R & Brzózka Z A microfluidic-based platform for tumour spheroid culture, monitoring and drug screening. Lab Chip 14, 2096–2104, doi:10.1039/c4lc00291a (2014). [PubMed: 24800721]
62. Lee SWL et al. Integrated in silico and 3D in vitro model of macrophage migration in response to physical and chemical factors in the tumor microenvironment. Integr Biol 12, 90–108, doi:10.1093/intbio/zyaa007 (2020).
63. Hwang H et al. Human breast cancer-derived soluble factors facilitate CCL19-induced chemotaxis of human dendritic cells. Sci Rep 6, 1–12, doi:10.1038/srep30207 (2016). [PubMed: 28442746]
64. Alexander S, Koehl GE, Hirschberg M, Geissler EK & Friedl P Dynamic imaging of cancer growth and invasion: a modified skin-fold chamber model. Histochem Cell Biol 130, 1147–1154, doi:10.1007/s00418-008-0529-1 (2008). [PubMed: 18987875]

65. Wolf K & Friedl P Extracellular matrix determinants of proteolytic and non-proteolytic cell migration. Trends Cell Biol 21, 736–744, doi:10.1016/j.tcb.2011.09.006 (2011). [PubMed: 22036198]
66. Bremer C, Tung CH & Weissleder R In vivo molecular target assessment of matrix metalloproteinase inhibition. Nat Med 7, 743–748, doi:10.1038/89126 (2001). [PubMed: 11385514]
67. Fisher KE et al. MT1-MMP- and Cdc42-dependent signaling co-regulate cell invasion and tunnel formation in 3D collagen matrices. J Cell Sci 122, 4558–4569, doi:10.1242/jcs.050724 (2009). [PubMed: 19934222]
68. Gaggioli C et al. Fibroblast-led collective invasion of carcinoma cells with differing roles for RhoGTPases in leading and following cells. Nat Cell Biol 9, 1392–1400, doi:10.1038/ncb1658 (2007). [PubMed: 18037882] Modeling and optical imaging to monitor and control cancer cell migration in co-cultures of cancer cells and stromal fibroblasts.
69. Wolf K et al. Collagen-based cell migration models in vitro and in vivo. Semin Cell Dev Biol 20, 931–941, doi:10.1016/j.semcdb.2009.08.005 (2009). [PubMed: 19682592]
70. Park D et al. High-throughput microfluidic 3D cytotoxicity assay for cancer immunotherapy (CACI-IMPACT platform). Front Immunol 10, 1133, doi:10.3389/fimmu.2019.01133 (2019). [PubMed: 31191524]
71. Wirtz D, Konstantopoulos K & Searson PC The physics of cancer: the role of physical interactions and mechanical forces in metastasis. Nat Rev Cancer 11, 512–522, doi:10.1038/nrc3080 (2011). [PubMed: 21701513]
72. Parlato S et al. 3D microfluidic model for evaluating immunotherapy efficacy by tracking dendritic cell behaviour toward tumor cells. Sci Rep 7, 1–16, doi:10.1038/s41598-017-01013-x (2017). [PubMed: 28127051]
73. Boussommier-Calleja A et al. The effects of monocytes on tumor cell extravasation in a 3D vascularized microfluidic model. Biomaterials 198, 180–193, doi:10.1016/j.biomaterials.2018.03.005 (2019). [PubMed: 29548546]
74. Binnewies M et al. Understanding the tumor immune microenvironment (TIME) for effective therapy. Nat Med 24, 541–550, doi:10.1038/s41591-018-0014-x (2018). [PubMed: 29686425]
75. Nguyen M et al. Dissecting effects of anti-cancer drugs and cancer-associated fibroblasts by on-chip reconstitution of immunocompetent tumor microenvironments. Cell Rep 25, 3884–3893. e3883, doi:10.1016/j.celrep.2018.12.015 (2018). [PubMed: 30590056] Micro-engineering approach to investigate intercellular interactions in the tumour microenvironment via single-cell tracking.
76. Yang X et al. Nanofiber membrane supported lung-on-a-chip microdevice for anti-cancer drug testing. Lab Chip 18, 486–495, doi:10.1039/c7lc01224a (2018). [PubMed: 29309077]
77. Collins T et al. Spheroid-on-chip microfluidic technology for the evaluation of the impact of continuous flow on metastatic potential in cancer models in vitro. Biomicrofluidics 15, 044103 (2021). [PubMed: 34504636]
78. Yi H-G et al. A bioprinted human-glioblastoma-on-a-chip for the identification of patient-specific responses to chemoradiotherapy. Nat Biomed Eng 3, 509–519, doi:10.1038/s41551-019-0363-x (2019). [PubMed: 31148598] Bioprinting tumor models to reflet complexity and heterogeneity in the tumor microenvironment.
79. Panagiotakopoulou M et al. Cell cycle–dependent force transmission in cancer cells. Mol Biol Cell 29, 2528–2539, doi:10.1091/mbc.E17-12-0726 (2018). [PubMed: 30113874]
80. Hansel CS et al. Nanoneedle-mediated stimulation of cell mechanotransduction machinery. ACS Nano 13, 2913–2926, doi:10.1021/acsnano.8b06998 (2019). [PubMed: 30829469]
81. Bergert M et al. Confocal reference free traction force microscopy. Nat Commun 7, 12814, doi:10.1038/ncomms12814 (2016). [PubMed: 27681958]
82. Zancla A, Mozetic P, Orsini M, Forte G & Rainer A A primer to traction force microscopy. J Biol Chem 298, 101867, doi:10.1016/j.jbc.2022.101867 (2022). [PubMed: 35351517]
83. Schaaf MB, Garg AD & Agostinis P Defining the role of the tumor vasculature in antitumor immunity and immunotherapy. Cell Death Dis 9, 1–14, doi:10.1038/s41419-017-0061-0 (2018). [PubMed: 29298988]

84. Ayuso JM et al. Evaluating natural killer cell cytotoxicity against solid tumors using a microfluidic model. Oncoimmunology 8, 1553477 (2019). [PubMed: 30723584]
85. Wimalachandra DC et al. Microfluidic-based immunomodulation of immune cells using upconversion nanoparticles in simulated blood vessel–tumor system. ACS Appl Mater Interfaces 11, 37513–37523, doi:10.1021/acsami.9b15178 (2019). [PubMed: 31547654]
86. Sohn LL et al. How can microfluidic and microfabrication approaches make experiments more physiologically relevant? Cell Syst 11, 209–211, doi:10.1016/j.cels.2020.07.003 (2020). [PubMed: 32888419]
87. Luque-González MA, Reis RL, Kundu SC & Caballero D Human microcirculation-on-chip models in cancer research: key integration of lymphatic and blood vasculatures. Adv Biosyst 4, 2000045, doi:10.1002/adbi.202000045 (2020).Micro-engineering approach that incorporates lymphatic and blood vasculatures in a tumor-on-a-chip platform.
88. Szklanny AA et al. 3D Bioprinting of engineered tissue flaps with hierarchical vessel networks (vesselnet) for direct host-to-implant perfusion. Adv Mater 33, 2102661, doi:10.1002/adma.202102661 (2021).
89. O'Connor C, Brady E, Zheng Y, Moore E & Stevens KR Engineering the multiscale complexity of vascular networks. Nat Rev Mater 7, 702–716, doi:10.1038/s41578-022-00447-8 (2022). [PubMed: 35669037]
90. Bocci F et al. Toward understanding cancer stem cell heterogeneity in the tumor microenvironment. Proc Natl Acad Sci U S A 116, 148–157, doi:10.1073/pnas.1815345116 (2019). [PubMed: 30587589]
91. Williams RM et al. Noninvasive ovarian cancer biomarker detection via an optical nanosensor implant. Sci Adv 4, eaaq1090, doi:10.1126/sciadv.aaq1090 (2021).
92. Perillo B et al. ROS in cancer therapy: the bright side of the moon. Exp Mol Med 52, 192–203, doi:10.1038/s12276-020-0384-2 (2020). [PubMed: 32060354]
93. Koch CJ Measurement of absolute oxygen levels in cells and tissues using oxygen sensors and 2-nitroimidazole EF5. Methods Enzymol 352, 3–31, doi:10.1016/s0076-6879(02)52003-6 (2002). [PubMed: 12125356]
94. Dranka BP et al. Assessing bioenergetic function in response to oxidative stress by metabolic profiling. Free Radic Biol Med 51, 1621–1635, doi:10.1016/j.freeradbiomed.2011.08.005 (2011). [PubMed: 21872656]
95. Smith AM, Mancini MC & Nie S Second window for in vivo imaging. Nat Nanotech 4, 710–711, doi:10.1038/nnano.2009.326 (2009).
96. Welsher K, Sherlock SP & Dai H Deep-tissue anatomical imaging of mice using carbon nanotube fluorophores in the second near-infrared window. Proc Natl Acad Sci U S A 108, 8943, doi:10.1073/pnas.1014501108 (2011). [PubMed: 21576494]
97. Mandal AK et al. Fluorescent sp^3 defect-tailored carbon nanotubes enable NIR-II single particle imaging in live brain slices at ultra-low excitation doses. Sci Rep 10, 5286, doi:10.1038/s41598-020-62201-w (2020). [PubMed: 32210295]
98. Heller DA et al. Peptide secondary structure modulates single-walled carbon nanotube fluorescence as a chaperone sensor for nitroaromatics. Proc Natl Acad Sci U S A 108, 8544–8549, doi:10.1073/pnas.1005512108 (2011). [PubMed: 21555544]
99. Heller DA et al. Multimodal optical sensing and analyte specificity using single-walled carbon nanotubes. Nat Nanotech 4, 114–120, doi:10.1038/nnano.2008.369 (2009).
100. Kim J-H et al. The rational design of nitric oxide selectivity in single-walled carbon nanotube near-infrared fluorescence sensors for biological detection. Nat Chem 1, 473–481, doi:10.1038/nchem.332 (2009). [PubMed: 21378915]
101. Zhang J et al. Single molecule detection of nitric oxide enabled by $d(AT)_{15}$ DNA adsorbed to near infrared fluorescent single-walled carbon nanotubes. J Am Chem Soc 133, 567–581, doi:10.1021/ja1084942 (2011). [PubMed: 21142158]
102. Jin H et al. Detection of single-molecule H_2O_2 signalling from epidermal growth factor receptor using fluorescent single-walled carbon nanotubes. Nat Nanotech 5, 302–309, doi:10.1038/nnano.2010.24 (2010).

103. Yaari Z et al. Nanoreporter of an enzymatic suicide inactivation pathway. Nano Lett 20, 7819–7827, doi:10.1021/acs.nanolett.0c01858 (2020). [PubMed: 33119310]
104. Zhao M et al. A tumor-microenvironment-responsive lanthanide–cyanine FRET sensor for nir-ii luminescence-lifetime in situ imaging of hepatocellular carcinoma. Adv Mater 32, 2001172, doi:10.1002/adma.202001172 (2020).
105. Li P et al. Quantifying the fast dynamics of HClO in living cells by a fluorescence probe capable of responding to oxidation and reduction events within the time scale of milliseconds. Anal Chem 92, 12987–12995, doi:10.1021/acs.analchem.0c01703 (2020). [PubMed: 32674559]
106. Zhao Q et al. Fluorescent/phosphorescent dual-emissive conjugated polymer dots for hypoxia bioimaging. Chem Sci 6, 1825–1831, doi:10.1039/C4SC03062A (2015). [PubMed: 28694947]
107. Jena PV et al. A carbon nanotube optical reporter maps endolysosomal lipid flux. ACS Nano 11, 10689–10703, doi:10.1021/acsnano.7b04743 (2017). [PubMed: 28898055]
108. Zhou K et al. Tunable, ultrasensitive pH-responsive nanoparticles targeting specific endocytic organelles in living cells. Angew Chem Intl Ed 50, 6109–6114, doi:10.1002/anie.201100884 (2011).
109. Ma X et al. Ultra-pH-sensitive nanoprobe library with broad pH tunability and fluorescence emissions. J Am Chem Soc 136, 11085–11092, doi:10.1021/ja5053158 (2014). [PubMed: 25020134]
110. Ma T et al. Dual-ratiometric target-triggered fluorescent probe for simultaneous quantitative visualization of tumor microenvironment protease activity and pH in vivo. J Am Chem Soc 140, 211–218, doi:10.1021/jacs.7b08900 (2018). [PubMed: 29237264] Multiplexed nanosensor technology to detect protease activity and pH in the tumor microenvironment.
111. Hou Y et al. Protease-activated ratiometric fluorescent probe for ph mapping of malignant tumors. ACS Nano 9, 3199–3205, doi:10.1021/acsnano.5b00276 (2015). [PubMed: 25670342]
112. Zhao T et al. A transistor-like pH nanoprobe for tumour detection and image-guided surgery. Nat Biomed Eng 1, 0006, doi:10.1038/s41551-016-0006 (2016). [PubMed: 28966871]
113. Voskuil FJ et al. Exploiting metabolic acidosis in solid cancers using a tumor-agnostic pH-activatable nanoprobe for fluorescence-guided surgery. Nat Commun 11, 3257, doi:10.1038/s41467-020-16814-4 (2020). [PubMed: 32591522]
114. Andreev OA, Engelman DM & Reshetnyak YK Targeting acidic diseased tissue: New technology based on use of the pH (Low) Insertion Peptide (pHLIP). Chim Oggi 27, 34–37 (2009). [PubMed: 20037661]
115. Andreev OA et al. pH (low) insertion peptide (pHLIP) inserts across a lipid bilayer as a helix and exits by a different path. Proc Natl Acad Sci U S A 107, 4081–4086, doi:10.1073/pnas.0914330107 (2010). [PubMed: 20160113]
116. Crawford T et al. pHLIP ICG for delineation of tumors and blood flow during fluorescence-guided surgery. Sci Rep 10, 18356, doi:10.1038/s41598-020-75443-5 (2020). [PubMed: 33110131] Nanosensor currently under clinical trial for image-guided surgery and other applications.
117. Bauer D et al. PET imaging of acidic tumor environment with ^{89}Zr-labeled pHLIP probes. Front Oncol 12, 882541, doi:10.3389/fonc.2022.882541 (2022). [PubMed: 35664740]
118. Kang B, Austin LA & El-Sayed MA Observing real-time molecular event dynamics of apoptosis in living cancer cells using nuclear-targeted plasmonically enhanced raman nanoprobes. ACS Nano 8, 4883–4892, doi:10.1021/nn500840x (2014). [PubMed: 24708404]
119. Li S-S et al. Monitoring the changes of pH in lysosomes during autophagy and apoptosis by plasmon enhanced Raman imaging. Anal Chem 91, 8398–8405, doi:10.1021/acs.analchem.9b01250 (2019). [PubMed: 31144810]
120. Guo J et al. Dynamic single-cell intracellular pH sensing using a SERS-active nanopipette. Analyst 145, 4852–4859, doi:10.1039/d0an00838a (2020). [PubMed: 32542257]
121. Jamieson LE et al. Targeted SERS nanosensors measure physicochemical gradients and free energy changes in live 3D tumor spheroids. Nanoscale 8, 16710–16718, doi:10.1039/C6NR06031E (2016). [PubMed: 27714168]

122. Chiappini C et al. Biodegradable nanoneedles for localized delivery of nanoparticles in vivo: Exploring the biointerface. ACS Nano 9, 5500–5509, doi:10.1021/acsnano.5b01490 (2015). [PubMed: 25858596]
123. Li Z & Zhang H Reprogramming of glucose, fatty acid and amino acid metabolism for cancer progression. Cell Mol Life Sci 73, 377–392, doi:10.1007/s00018-015-2070-4 (2016). [PubMed: 26499846]
124. Leone Robert D et al. Glutamine blockade induces divergent metabolic programs to overcome tumor immune evasion. Science 366, 1013–1021, doi:10.1126/science.aav2588 (2019). [PubMed: 31699883]
125. Lau AN & Vander Heiden MG Metabolism in the tumor microenvironment. Annu Rev Cancer Biol 4, 17–40, doi:10.1146/annurev-cancerbio-030419-033333 (2020).
126. US National Library of Medicine. ClinicalTrials.gov, https://ClinicalTrials.gov/show/NCT04473378 (2019).
127. Nascimento RAS et al. Single cell “glucose nanosensor” verifies elevated glucose levels in individual cancer cells. Nano Lett 16, 1194–1200, doi:10.1021/acs.nanolett.5b04495 (2016). [PubMed: 26752097]
128. Ma Z et al. In-situ monitoring of glucose metabolism in cancer cell microenvironments based on hollow fiber structure. Biosens Bioelectron 162, 112261, doi:10.1016/j.bios.2020.112261 (2020). [PubMed: 32392160]
129. Actis P et al. Compartmental genomics in living cells revealed by single-cell nanobiopsy. ACS Nano 8, 546–553, doi:10.1021/nn405097u (2014). [PubMed: 24279711]
130. Nashimoto Y et al. Evaluation of mRNA localization using double barrel scanning ion conductance microscopy. ACS Nano 10, 6915–6922, doi:10.1021/acsnano.6b02753 (2016). [PubMed: 27399804]
131. Damaghi M et al. Chronic acidosis in the tumour microenvironment selects for overexpression of LAMP2 in the plasma membrane. Nat Commun 6, 8752, doi:10.1038/ncomms9752 (2015). [PubMed: 26658462]
132. Hui S et al. Glucose feeds the TCA cycle via circulating lactate. Nature 551, 115–118, doi:10.1038/nature24057 (2017). [PubMed: 29045397]
133. Brand A et al. DHA-associated lactic acid production blunts tumor immunosurveillance by T and NK cells. Cell Metab 24, 657–671, doi:10.1016/j.cmet.2016.08.011 (2016). [PubMed: 27641098]
134. Cali JJ et al. Compounds and methods for assaying redox state of metabolically active cells and methods for measuring NAD(P)/NAD(P)H. United States patent (2016).
135. Zheng XT, Yang HB & Li CM Optical detection of single cell lactate release for cancer metabolic analysis. Anal Chem 82, 5082–5087, doi:10.1021/ac100074n (2010). [PubMed: 20469833]
136. Jena BK & Raj CR Electrochemical biosensor based on integrated assembly of dehydrogenase enzymes and gold nanoparticles. Anal Chem 78, 6332–6339, doi:10.1021/ac052143f (2006). [PubMed: 16970306]
137. Xu Y-T et al. A practical electrochemical nanotool for facile quantification of amino acids in single cell. Small 17, 2100503, doi:10.1002/smll.202100503 (2021).
138. Snaebjornsson MT, Janaki-Raman S & Schulze A Greasing the wheels of the cancer machine: The role of lipid metabolism in cancer. Cell Metab 31, 62–76, doi:10.1016/j.cmet.2019.11.010 (2020). [PubMed: 31813823]
139. Broadfield LA, Pane AA, Talebi A, Swinnen JV & Fendt S-M Lipid metabolism in cancer: New perspectives and emerging mechanisms. Dev Cell 56, 1363–1393, doi:10.1016/j.devcel.2021.04.013 (2021). [PubMed: 33945792]
140. Mancini R et al. Metabolic features of cancer stem cells: the emerging role of lipid metabolism. Oncogene 37, 2367–2378, doi:10.1038/s41388-018-0141-3 (2018). [PubMed: 29445137]
141. Hendrikx T, Walenbergh SMA, Hofker MH & Shiri-Sverdlov R Lysosomal cholesterol accumulation: driver on the road to inflammation during atherosclerosis and non-alcoholic steatohepatitis. Obesity Rev 15, 424–433, doi:10.1111/obr.12159 (2014).
142. Michelotti GA, Machado MV & Diehl AM NAFLD, NASH and liver cancer. Nat Rev Gastroenterol Hepatol 10, 656–665, doi:10.1038/nrgastro.2013.183 (2013). [PubMed: 24080776]

143. Mehlem A, Hagberg CE, Muhl L, Eriksson U & Falkevall A Imaging of neutral lipids by oil red O for analyzing the metabolic status in health and disease. Nat Protoc 8, 1149–1154, doi:10.1038/nprot.2013.055 (2013). [PubMed: 23702831]
144. Hofmann K et al. A novel alkyne cholesterol to trace cellular cholesterol metabolism and localization. J Lipid Res 55, 583–591, doi:10.1194/jlr.D044727 (2014). [PubMed: 24334219]
145. Takatori S, Mesman R & Fujimoto T Microscopic methods to observe the distribution of lipids in the cellular membrane. Biochemistry 53, 639–653, doi:10.1021/bi401598v (2014). [PubMed: 24460209]
146. Mondal S, Rakshit A, Pal S & Datta A Cell permeable ratiometric fluorescent sensors for imaging phosphoinositides. ACS Chem Biol 11, 1834–1843, doi:10.1021/acschembio.6b00067 (2016). [PubMed: 27082310]
147. Galassi TV et al. An optical nanoreporter of endolysosomal lipid accumulation reveals enduring effects of diet on hepatic macrophages in vivo. Sci Transl Med 10, doi:10.1126/scitranslmed.aar2680 (2018).
148. Yong C, Stewart GD & Frezza C Oncometabolites in renal cancer. Nat Rev Nephrol 16, 156–172, doi:10.1038/s41581-019-0210-z (2020). [PubMed: 31636445]
149. Liu Y & Yang C Oncometabolites in cancer: Current understanding and challenges. Cancer Res 81, 2820–2823, doi:10.1158/0008-5472.CAN-20-3730 (2021). [PubMed: 33762356]
150. Yang M, Soga T & Pollard PJ Oncometabolites: Linking altered metabolism with cancer. J Clin Invest 123, 3652–3658, doi:10.1172/jci67228 (2013). [PubMed: 23999438]
151. Kaper T et al. Nanosensor detection of an immunoregulatory tryptophan influx/kynurenine efflux cycle. PLOS Biol 5, e257, doi:10.1371/journal.pbio.0050257 (2007). [PubMed: 17896864]
152. Fehr M, Lalonde S, Lager I, Wolff MW & Frommer WB In vivo imaging of the dynamics of glucose uptake in the cytosol of COS-7 cells by fluorescent nanosensors. J Biol Chem 278, 19127–19133, doi:10.1074/jbc.M301333200 (2003). [PubMed: 12649277]
153. Zhang J et al. Molecular recognition using corona phase complexes made of synthetic polymers adsorbed on carbon nanotubes. Nat Nanotech 8, 959–968, doi:10.1038/nnano.2013.236 (2013).Strategy to develop optical nanosensors based on synthetic molecular recognition.
154. Amir D, Hendler-Neumark A, Wulf V, Ehrlich R & Bisker G Oncometabolite fingerprinting using fluorescent single-walled carbon nanotubes. Adv Mater Interfaces 9, 2101591, doi:10.1002/admi.202101591 (2022).
155. Ježek P 2-Hydroxyglutarate in cancer cells. Antioxid Redox Signal 33, 903–926, doi:10.1089/ars.2019.7902 (2020). [PubMed: 31847543]
156. Ehrlich R, Hendler-Neumark A, Wulf V, Amir D & Bisker G Optical nanosensors for real-time feedback on insulin secretion by β-cells. Small 17, 2101660, doi:10.1002/smll.202101660 (2021).
157. Levy JMM, Towers CG & Thorburn A Targeting autophagy in cancer. Nat Rev Cancer 17, 528–542, doi:10.1038/nrc.2017.53 (2017). [PubMed: 28751651]
158. Linder B & Kögel D Autophagy in cancer cell death. Biology 8 (2019).
159. Huefner A et al. Characterization and visualization of vesicles in the endo-lysosomal pathway with surface-enhanced Raman spectroscopy and chemometrics. ACS Nano 10, 307–316, doi:10.1021/acsnano.5b04456 (2016). [PubMed: 26649752]
160. Chen Z et al. Single gold@silver nanoprobes for real-time tracing the entire autophagy process at single-cell level. J Am Chem Soc 137, 1903–1908, doi:10.1021/ja5112628 (2015). [PubMed: 25606663]
161. Ou Y-C, Wen X & Bardhan R Cancer immunoimaging with smart nanoparticles. Trends Biotechnol 38, 388–403, doi:10.1016/j.tibtech.2019.11.001 (2020). [PubMed: 31812371]
162. Dauphin-Ducharme P et al. Electrochemical aptamer-based sensors for improved therapeutic drug monitoring and high-precision, feedback-controlled drug delivery. ACS Sensors 4, 2832–2837, doi:10.1021/acssensors.9b01616 (2019). [PubMed: 31556293]
163. Arroyo-Currás N et al. Real-time measurement of small molecules directly in awake, ambulatory animals. Proc Natl Acad Sci U S A 114, 645–650, doi:10.1073/pnas.1613458114 (2017). [PubMed: 28069939]

164. Parolo C et al. Real-time monitoring of a protein biomarker. ACS Sensors 5, 1877–1881, doi:10.1021/acssensors.0c01085 (2020). [PubMed: 32619092]
165. Zheng A et al. CD16/PD-L1 bi-specific aptamer for cancer immunotherapy through recruiting NK cells and acting as immunocheckpoint blockade. Mol Ther Nucleic 27, 998–1009, doi:10.1016/j.omtn.2022.01.010 (2022).
166. Cui D, Li J, Zhao X, Pu K & Zhang R Semiconducting polymer nanoreporters for near-infrared chemiluminescence imaging of immunoactivation. Adv Mater 32, 1906314, doi:10.1002/adma.201906314 (2020).
167. Dheer D, Nicolas J & Shankar R Cathepsin-sensitive nanoscale drug delivery systems for cancer therapy and other diseases. Adv Drug Deliv Rev 151–152, 130–151, doi:10.1016/j.addr.2019.01.010 (2019).
168. Shahriari M et al. Enzyme responsive drug delivery systems in cancer treatment. J Control Release 308, 172–189, doi:10.1016/j.jconrel.2019.07.004 (2019). [PubMed: 31295542]
169. Vizovisek M, Ristanovic D, Menghini S, Christiansen MG & Schuerle S The tumor proteolytic landscape: A challenging frontier in cancer diagnosis and therapy. Int J Mol Sci 22, 2514, doi:10.3390/ijms22052514 (2021). [PubMed: 33802262]
170. Bengsch F et al. Cell type-dependent pathogenic functions of overexpressed human cathepsin B in murine breast cancer progression. Oncogene 33, 4474–4484, doi:10.1038/onc.2013.395 (2014). [PubMed: 24077280]
171. Scott JI, Deng Q & Vendrell M Near-infrared fluorescent probes for the detection of cancer-associated proteases. ACS Chem Biol 16, 1304–1317, doi:10.1021/acschembio.1c00223 (2021). [PubMed: 34315210]
172. Kwon EJ, Dudani JS & Bhatia SN Ultrasensitive tumour-penetrating nanosensors of protease activity. Nat Biomed Eng 1, 0054, doi:10.1038/s41551-017-0054 (2017). [PubMed: 28970963] Development of optical nanosensors that are selectively activated by tumour-specific protease to detect small tumours.
173. Dudani JS, Jain PK, Kwong GA, Stevens KR & Bhatia SN Photoactivated spatiotemporally-responsive nanosensors of in vivo protease activity. ACS Nano 9, 11708–11717, doi:10.1021/acsnano.5b05946 (2015). [PubMed: 26565752]
174. Myochin T et al. Development of a series of near-infrared dark quenchers based on Si-rhodamines and their application to fluorescent probes. J Am Chem Soc 137, 4759–4765, doi:10.1021/jacs.5b00246 (2015). [PubMed: 25764154]
175. Fernald K & Kurokawa M Evading apoptosis in cancer. Trends Cell Biol 23, 620–633, doi:10.1016/j.tcb.2013.07.006 (2013). [PubMed: 23958396]
176. Liu C et al. A graphene oxide nanosensor enables the co-delivery of aptamer and peptide probes for fluorescence imaging of a cascade reaction in apoptotic signaling. Analyst 143, 208–214, doi:10.1039/C7AN01515A (2018).
177. Zhang X et al. A fluorescent turn on nanoprobe for simultaneous visualization of dual-targets involved in cell apoptosis and drug screening in living cells. Nanoscale 9, 10861–10868, doi:10.1039/C7NR03564K (2017). [PubMed: 28731107]
178. Sindhwani S et al. The entry of nanoparticles into solid tumours. Nat Mater 19, 566–575, doi:10.1038/s41563-019-0566-2 (2020). [PubMed: 31932672]
179. Wilhelm S et al. Analysis of nanoparticle delivery to tumours. Nat Rev Mater 1, 16014, doi:10.1038/natrevmats.2016.14 (2016).
180. Christian S et al. Nucleolin expressed at the cell surface is a marker of endothelial cells in angiogenic blood vessels. J Cell Biol 163, 871–878, doi:10.1083/jcb.200304132 (2003). [PubMed: 14638862]
181. Safaee MM, Gravely M & Roxbury D A wearable optical microfibrous biomaterial with encapsulated nanosensors enables wireless monitoring of oxidative stress. Adv Healthc Mater 31, 2006254, doi:10.1002/adfm.202006254 (2021).
182. Harvey JD et al. A carbon nanotube reporter of microRNA hybridization events in vivo. Nat Biomed Eng 1, 0041, doi:10.1038/s41551-017-0041 (2017). [PubMed: 28845337] Minimally invasive implantable sensor technology to longitudinally monitor tumour biomarkers in vivo.

183. Williams RM et al. Noninvasive ovarian cancer biomarker detection via an optical nanosensor implant. Sci Adv 4, eaaq1090, doi:10.1126/sciadv.aaq1090 (2021).

184. Horowitz L et al. Multiplexed drug testing of tumor slices using a microfluidic platform. NPJ Precis Oncol 4, 12, doi:10.1038/s41698-020-0117-y (2020). [PubMed: 32435696]

185. Wong BS et al. A microfluidic cell-migration assay for the prediction of progression-free survival and recurrence time of patients with glioblastoma. Nat Biomed Eng 5, 26–40, doi:10.1038/s41551-020-00621-9 (2021). [PubMed: 32989283]

186. Kim M et al. Detection of ovarian cancer via the spectral fingerprinting of quantum-defect-modified carbon nanotubes in serum by machine learning. Nat Biomed Eng 6, 267–275, doi:10.1038/s41551-022-00860-y (2022). [PubMed: 35301449]

187. Phillips E et al. Clinical translation of an ultrasmall inorganic optical-PET imaging nanoparticle probe. Sci Transl Med 6, 260ra149–260ra149, doi:10.1126/scitranslmed.3009524 (2014).

188. Serkova NJ Nanoparticle-based magnetic resonance imaging on tumor-associated macrophages and inflammation. Front Immunol 8, 590–590, doi:10.3389/fimmu.2017.00590 (2017). [PubMed: 28588582]

189. Guo J et al. Auto-affitech: An automated ligand binding affinity evaluation platform using digital microfluidics with a bidirectional magnetic separation method. Lab Chip 20, 1577–1585, doi:10.1039/d0lc00024h (2020). [PubMed: 32207498]

190. Song JW et al. Microfluidic endothelium for studying the intravascular adhesion of metastatic breast cancer cells. PLOS ONE 4, e5756, doi:10.1371/journal.pone.0005756 (2009). [PubMed: 19484126]

191. Eduati F et al. A microfluidics platform for combinatorial drug screening on cancer biopsies. Nat Commun 9, 2434, doi:10.1038/s41467-018-04919-w (2018). [PubMed: 29934552]

192. Aref AR et al. Screening therapeutic EMT blocking agents in a three-dimensional microenvironment. Integr Biol (Camb) 5, 381–389, doi:10.1039/c2ib20209c (2013). [PubMed: 23172153]

193. Zhao S-P et al. Three-dimensional cell culture and drug testing in a microfluidic sidewall-attached droplet array. Anal Chem 89, 10153–10157, doi:10.1021/acs.analchem.7b02267 (2017). [PubMed: 28885822]

194. Shang M et al. Microfluidic studies of hydrostatic pressure-enhanced doxorubicin resistance in human breast cancer cells. Lab Chip 21, 746–754, doi:10.1039/d0lc01103g (2021). [PubMed: 33502419]

195. Hassell BA et al. Human organ chip models recapitulate orthotopic lung cancer growth, therapeutic responses, and tumor dormancy in vitro. Cell Rep 21, 508–516, doi:10.1016/j.celrep.2017.09.043 (2017). [PubMed: 29020635]

196. Ying L et al. Cancer associated fibroblast-derived hepatocyte growth factor inhibits the paclitaxel-induced apoptosis of lung cancer A549 cells by up-regulating the PI3K/Akt and GRP78 signaling on a microfluidic platform. PLOS ONE 10, e0129593, doi:10.1371/journal.pone.0129593 (2015). [PubMed: 26115510]

197. Niidome Y, Wakabayashi R, Goto M, Fujigaya T & Shiraki T Protein-structure-dependent spectral shifts of near-infrared photoluminescence from locally functionalized single-walled carbon nanotubes based on avidin–biotin interactions. Nanoscale, doi:10.1039/D2NR01440H (2022).

198. Kwon H et al. Optical probing of local pH and temperature in complex fluids with covalently functionalized, semiconducting carbon nanotubes. J Phys Chem C 119, 3733–3739, doi:10.1021/jp509546d (2015).

199. Zeng W et al. Ratiometric imaging of MMP-2 activity facilitates tumor detection using activatable near-infrared fluorescent semiconducting polymer nanoparticles. Small 17, 2101924, doi:10.1002/smll.202101924 (2021).

200. Tavaré R et al. An effective immuno-PET imaging method to monitor CD8-dependent responses to immunotherapy. Cancer Res 76, 73–82, doi:10.1158/0008-5472.CAN-15-1707 (2016). [PubMed: 26573799]

201. Dai X, Zhou W, Gao T, Liu J & Lieber CM Three-dimensional mapping and regulation of action potential propagation in nanoelectronics-innervated tissues. Nat Nanotech 11, 776–782, doi:10.1038/nnano.2016.96 (2016).
202. Sontheimer-Phelps A, Hassell BA & Ingber DE Modelling cancer in microfluidic human organs-on-chips. Nat Rev Cancer 19, 65–81, doi:10.1038/s41568-018-0104-6 (2019). [PubMed: 30647431]
203. US National Library of Medicine. ClinicalTrials.gov, https://ClinicalTrials.gov/show/NCT04996355 (2021).
204. US National Library of Medicine. ClinicalTrials.gov, https://ClinicalTrials.gov/show/NCT04755907 (2021).
205. US National Library of Medicine. ClinicalTrials.gov, https://ClinicalTrials.gov/show/NCT05130801 (2021).
206. Daldrup-Link HE et al. MRI of tumor-associated macrophages with clinically applicable iron oxide nanoparticles. Clin Cancer Res 17, 5695–5704, doi:10.1158/1078-0432.CCR-10-3420 (2011). [PubMed: 21791632]
207. US National Library of Medicine. ClinicalTrials.gov, https://ClinicalTrials.gov/show/NCT04682847 (2020).
208. Anselmo AC & Mitragotri S Nanoparticles in the clinic: An update post COVID-19 vaccines. Bioeng Transl Med 6, e10246, doi:10.1002/btm2.10246 (2021). [PubMed: 34514159]
209. Benezra M et al. Multimodal silica nanoparticles are effective cancer-targeted probes in a model of human melanoma. J Clin Investig 121, 2768–2780, doi:10.1172/JCI45600 (2011). [PubMed: 21670497]
210. US National Library of Medicine. ClinicalTrials.gov, https://ClinicalTrials.gov/show/NCT02106598 (2014).
211. Martin KH & Dayton PA Current status and prospects for microbubbles in ultrasound theranostics. Wiley Interdiscip Rev Nanomed Nanobiotechnol 5, 329–345, doi:10.1002/wnan.1219 (2013). [PubMed: 23504911]
212. US National Library of Medicine. ClinicalTrials.gov, https://ClinicalTrials.gov/show/NCT03199274 (2017).
213. Manzari MT et al. Targeted drug delivery strategies for precision medicines. Nat Rev Mater 6, 351–370, doi:10.1038/s41578-020-00269-6 (2021). [PubMed: 34950512]
214. Mitchell MJ et al. Engineering precision nanoparticles for drug delivery. Nat Rev Drug Discov 20, 101–124, doi:10.1038/s41573-020-0090-8 (2021). [PubMed: 33277608]
215. Gurbatri CR, Arpaia N & Danino T Engineering bacteria as interactive cancer therapies. Science 378, 858–864, doi:10.1126/science.add9667 (2022). [PubMed: 36423303]
216. Li C & Samulski RJ Engineering adeno-associated virus vectors for gene therapy. Nat Rev Genet 21, 255–272, doi:10.1038/s41576-019-0205-4 (2020). [PubMed: 32042148]
217. Shipman SL, Nivala J, Macklis JD & Church GM Molecular recordings by directed CRISPR spacer acquisition. Science 353, aaf1175, doi:doi:10.1126/science.aaf1175 (2016).

Box 1 |

Engineering technologies in clinical translation.

Multiple classes of micro- and nanotechnologies have reached the clinic. Drug screening platforms using micro- or nanoengineered technologies are in clinical use. Patient-derived tumour slices on microfluidic devices have been developed for multiplexed drug testing in glioblastoma and metastatic colorectal cancer.[184] Cell-based microfluidic assays have been tested for combinatorial drug screening using a single-cell suspension created from pancreatic tumour biopsies.[191] Such microfluidic platforms have enabled rapid screening of drugs and dose optimization, requiring smaller amounts of patient samples and drugs than conventional well plate-based assays.[202] To personalize treatment options in the clinic, patient-derived organoids-on-a-chip have been tested to screen drugs via microfluidic chip-based assay, compare the results of patient's medication regimen, and assess response to guide colorectal cancer treatment (NCT04996355).[203] Bioprinted 3D tumor models have demonstrated the potential to assist in the development of personalized anticancer therapies, including preclinical drug screening and the prediction of patient treatment response.[13,23] Patient-derived colorectal cancer tissues have been employed to establish a 3D bioprinted model and to predict clinical efficacy of chemotherapeutic drugs (NCT04755907).[204]

A handful of nanoscale contrast agents have progressed to clinical trials as key breakthroughs for diagnostics and in vivo imaging. The near-infrared fluorophore-labeled pH-responsive peptide enables high contrast, resolution, and sensitivity imaging of tumors *in vivo* and has demonstrated great potential for imaging-guided tumour resection in breast cancer (NCT05130801).[205] A recently reported human trial on superparamagnetic iron oxide nanoparticles (SPIONs) was used to non-invasively image tumour-associated macrophages using MRI (NCT04682847).[188,206,207] As the density of tumour-associated macrophages in many solid tumours indicates the severity of the inflammatory microenvironment, SPIONs offer key diagnostic information that correlates to clinical outcomes for chemotherapy or radiotherapy.[188,208] C-dots are a class of silica-based nanoparticles that have been used for multimodal (PET and fluorescence) tumor imaging. Surface conjugation of the tumor-specific antibody fragments or peptides enables the targeted delivery.[187,209] C-dots labelled with ^{124}I for PET imaging and functionalized with an integrin-targeting peptide, cyclo-(Arg-Gly-Asp-Tyr), have been used to detect integrin-expressing cancers and are in trials for imaging melanoma, malignant brain tumours, and oral cavity squamous cell carcinoma (NCT02106598).[210] C-dots also display a high level of safety and pharmacokinetics profile attributed to their ultra-small size (<10 nm). Compared to nanosensors larger than 10nm, C-dots are readily cleared through renal pathways and minilize uptake by reticuloendothelial systems. Perflutren Protein-Type A Microspheres are gas-filled particles used as ultrasound contrast agents in clinics (NCT03199274).[211,212] The microspheres vibrate and re-emit backscatter ultrasound that is distinct from the surrounding tissues. Proteins, lipids, and surfactants can further stabilize the microspheres to circulate in the blood, and further functionalization of ligands can accumulate microspheres at the disease sites, for example in liver cancer.

Many drug delivery technologies are approved or in trials, and they are reviewed elsewhere.[213,214]

Box 2 |

Combining nanotechnologies with genetic engineering and synthetic biology

The combination of genetic engineering or synthetic biology approaches with nanotechnological techniques can help expand the tools available to understand the in vivo dynamics of protein expression and/or genetic alteration. For instance, these approaches could be used to produce hybrid virus- or bacteria-like particles that can make "decisions" based on biological inputs, such as activation of a receptor followed by the functional output of a nanoparticle (i.e., drug release) downstream.[215,216] Such hybrid particles could be spatiotemporally controlled by external inputs such as magnetic fields, tissue-penetrating light, or infusion of chemicals. This would enable "return missions" by the particles to tumours to collect biospecimens, measure biochemical properties, or perhaps record biological processes such as signalling events or dwell time of specific cell types over time into DNA-based recorders – conceptually much like wildlife cameras are used to examine the behaviour of animals in the wild. Multimodal CRISPR-based recorders capable of storing complex information, such as movies, have been developed and applied in bacteria.[217] In addition, different types of hybrid particles could be used in a cooperative network, information is synthesized by particles that sense not only specific aspects of the tumour ecosystem but also one another to make decisions.[215] Examples of such scenarios would include release of immunostimulatory drugs only in the presence of specific immune cell types, cytokines, and/or target cells or emission of FRET spectra reporting proximity of two or more cell types within the tumour. These types of active diagnostics will enable phenotyping of tumours and monitoring of drug responses at unprecedented resolution, which may lead to new opportunities in personalized medicine.

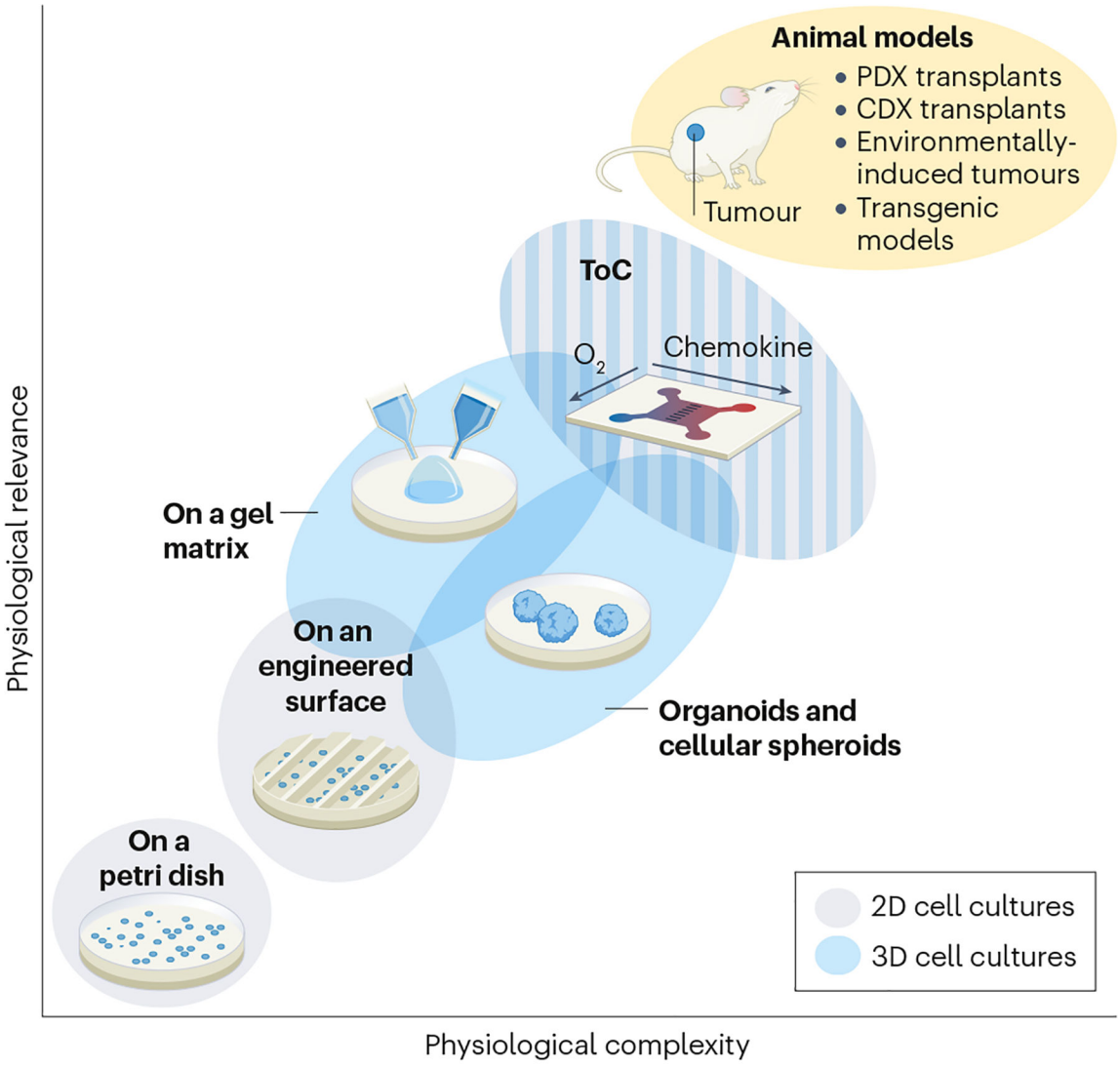

Figure 1 |. Preclinical models of tumour ecosystems.

Preclinical tumour models with variable dimensionality, biological complexity and physiological relevance fulfil different requirements to study tumour ecosystems. Building upon the simplest two-dimensional (2D) cell-culture technique, micro- or nano-engineered surface matrices are introduced to recapitulate complex cell–cell and cell–extracellular matrix (ECM) interactions, respectively. Three-dimensional (3D) cell culture models, including multicellular organoids, spheroids, and 3D cell cultures bioprinted on gel matrices, increase the physiological relevance and complexity of studies to better capture a solid tumour environment. Tumour-on-a-chip (ToC) approach increased the controllable and customizable parameters in different analytes that better mimic the TME and are able to illustrate complex interactions between tumour and environments. *In vivo* murine models can closely recapitulate tumour ecosystems with high physiological relevance and complexity, such as human patient-derived xenografts (PDX), cell-derived xenograft (CDX), environmentally-induced model (carcinogen or environmental factors exposure to induce cancer development), and genetically-engineered mouse models (GEMM). Although the

complexity and heterogeneity make the in vivo murine models challenging to pinpoint the ecosystem dynamics with spatiotemporal details, micro- and nano-engineering aims to reach a similar level of physiological relevance and complexity but with controllable parameters. The blue ovals correspond to the variability of dimension and biological complexity for each model system.

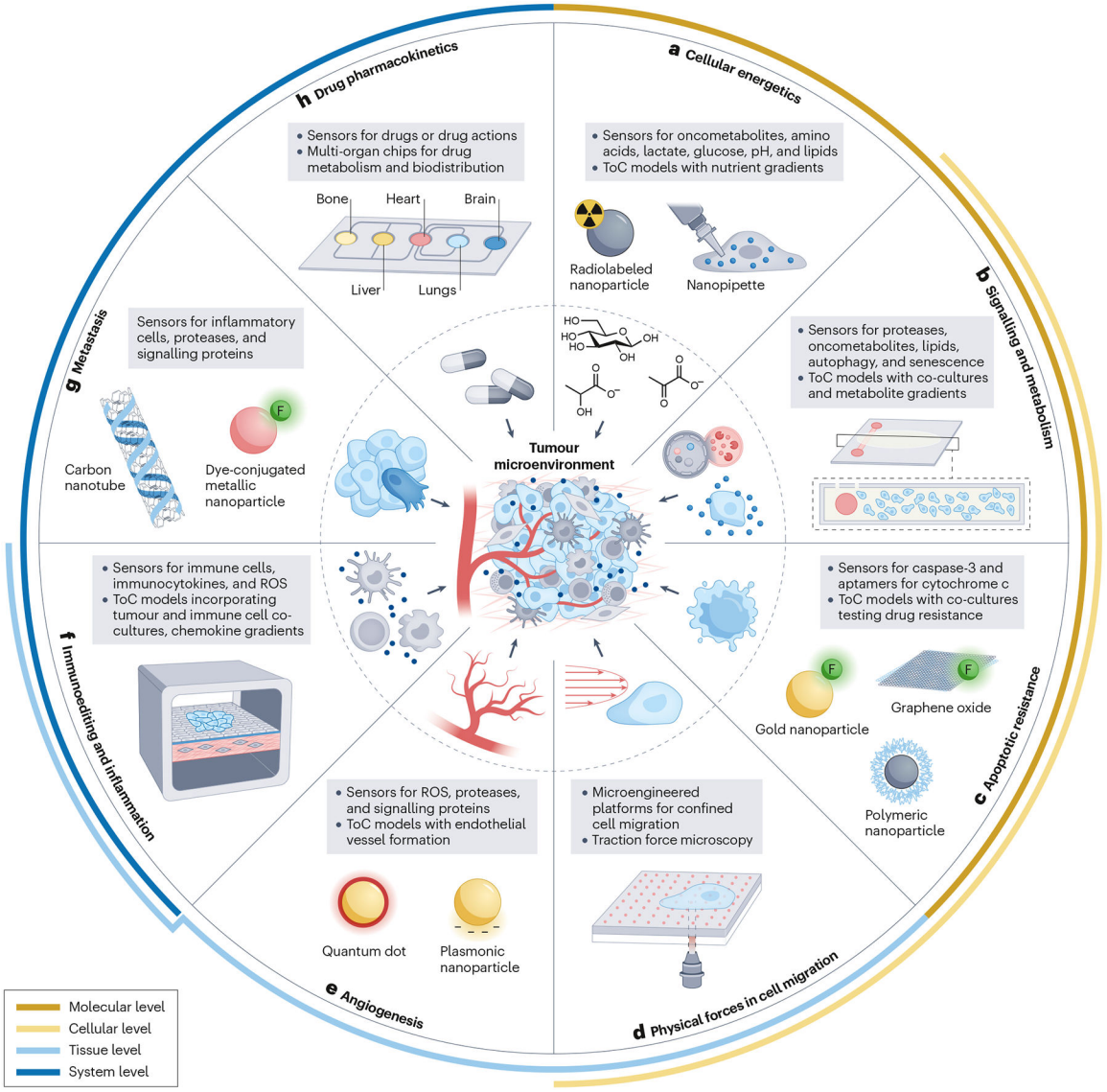

Figure 2 |. Research tools to investigate hallmark processes and bioanalytes in tumour ecosystems.

Tumour cells undergo extensive cellular and molecular crosstalk with the immediate niche and distant organs to achieve homeostasis in their ecosystems. Cancer hallmarks like cellular energetics (**a**), proliferative signalling and cancer cell metabolism (**b**), apoptotic resistance (**c**), physical and structural components of the tumour microenvironment (TME) (**d**), angiogenesis (**e**), inflammation and immunoediting (**f**), to metastasis (**g**) or systemic drug responses (**h**) are important to characterize at every stage of tumourigenesis and progression. Technologies including nanosensors and ToC models have been developed to precisely monitor and mimic the complex biological processes occurring in tumour ecosystems. These micro- and nanoscale engineering approaches capture unique features of tumours and TME and provide novel insights for tumour development. Images in the inner circle represent related biological processes and analytes. The outer circle lists illustrative examples of nanoscale approaches to monitor or model them.

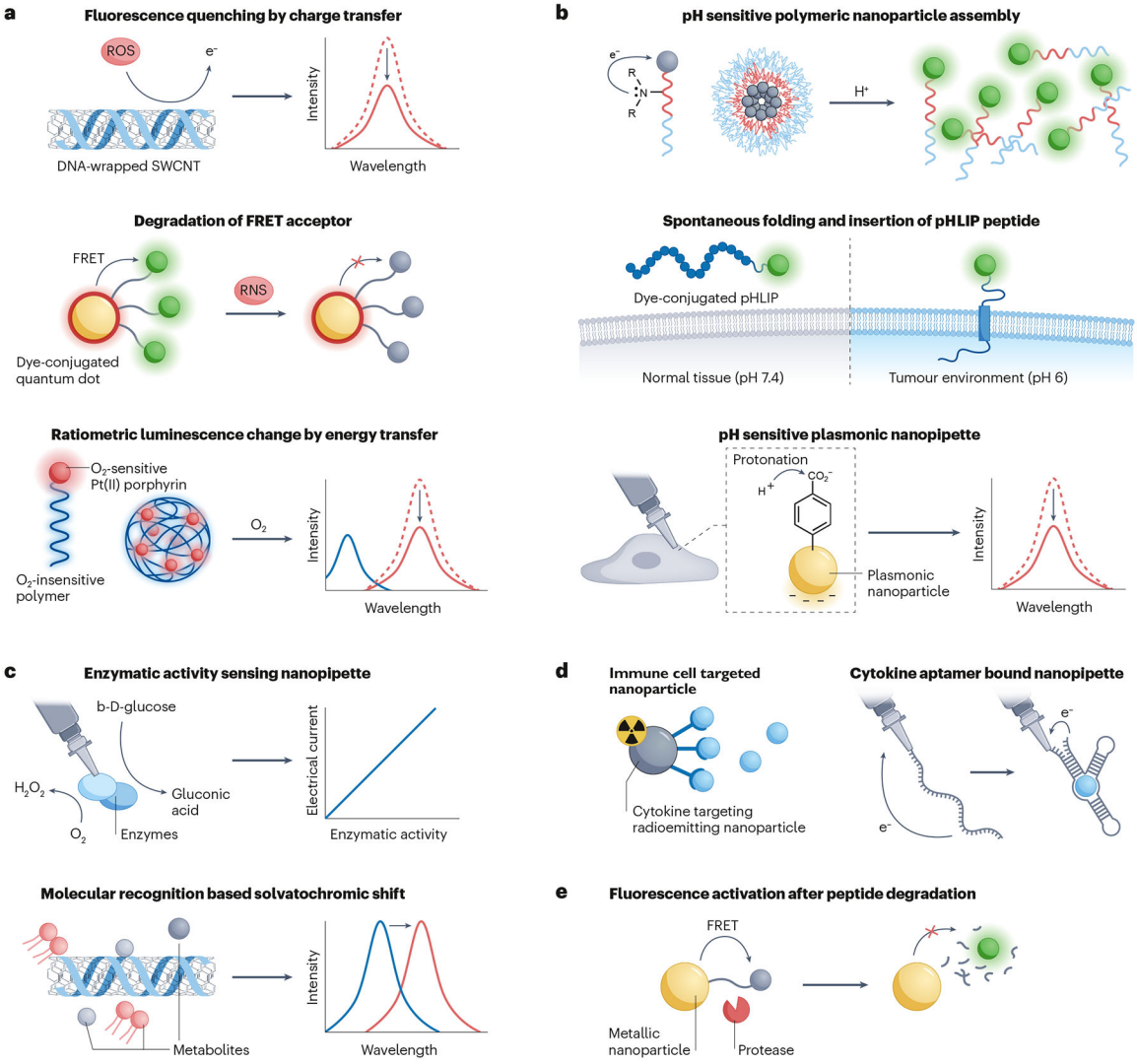

Figure 3 |. Nanosensor technologies to investigate tumour ecosystems.

a | Reactive oxygen species (ROS), reactive nitrogen species (RNS), and oxygen level can be detected based on fluorescence quenching in single-walled carbon nanotubes (SWCNT), reduction of FRET efficiency in dye-conjugated quantum dots, or ratiometric luminescence change in oxygen-sensitive polymeric nanoparticle, respectively. **b** | pH-sensing nanosensors largely use the functionalization of protonatable functional groups, such as amine and carboxyl groups. Dye-labelled pH-low insertion peptide (pHLIP) spontaneously folds and inserts across cell membranes at low pH, enabling sensitive optical imaging of cells in acidic tumour tissues. Protonation of the functional group at low pH decreases the surface-enhanced Raman spectroscopy (SERS) signal in plasmonic nanopipettes and photoinduced electron transfer from tertiary amine to dye in polymeric nanoparticles, activating dye fluorescence. **c** | Metabolite-sensing nanopipettes can be coupled with an enzyme that reacts with the metabolite of interest or cofactor, transducing electrochemical signals by enzymatic reactions. Diverse physicochemical interactions between SWCNT and metabolites can alter the dielectric environment of SWCNT and generate a fluorescence wavelength or intensity

shift. **d** | Immuno-nanosensors are constructed by conjugation of nanoparticles with cytokine binding proteins or aptamers. Cytokine-specific bindings can change the electrochemical signals of a nanopipette or enable localization of radioemitting nanoparticles in the tumour microenvironment (TME). **e** | Protease-specific nanosensors are conjugated with peptides and detect protease-cleavage events based on the reduction of FRET efficiency of dye-conjugated metallic nanoparticles.

Table 1 |

Nano- and microengineering approaches for therapeutic target discovery and modulation

Model setup	Advantages	Outcome	Ref
Target selection			
Droplet-based microfluidic chip for single-cell RT-PCR	High-throughput; Streamlined workflow that integrates cell lysis and reagent addition into one device	Faster and reliable processing for single-cell RT-PCR	10
Droplet-based microfluidics for ligand-binding affinity evaluation	Rapid incubation and separation of target beads and binding ligands	Identification of dissociation constants of the antigen EpCAM and its corresponding aptamer, SYL3C	189
Microfluidic vasculature system for target identification	Recreation of physiological dynamic flow conditions and circulation of metastatic breast cancer cells in the vascular channel	Identification of inhibition of CXCL12–CXCR4 binding on endothelial cells as a therapeutic target for breast cancer metastasis	190
Lead identification			
Microfluidics platform for combinational drug screening on cancer biopsies	Minimal reagent and tissue consumption; Screening of cells from patient tumours without need for ex vivo culturing steps	Identification of potential synergistic effect between PHT-427 and selumetinib; Drug-induced toxicity screening	191
Tumor cell spheroids in a 3D hydrogel scaffold assay for drug screening	Co-culture; Recapitulate epithelial–mesenchymal transition-induced tumour dispersion and endothelial cell-dependent phenotypic changes in cancer cells	Closer approximations of drug efficacy in humans measured during clinical trials than prediction by 2D and/or monoculture models.	192
Preclinical studies			
Droplet-based 3D cell culture model using nanolitre-scale droplets in a microfluidic chip	High-throughput; Miniaturized platform for 3D cell culture; Better control to spheroid sizes and flows in spatiotemporal domains	Higher resistance of HepG2 cells to doxorubicin in 3D than 2D models	193
Multiplexed drug testing of intact cancer slice cultures from xenograft or patients	High-throughput; Real patient tissue testing	Differential responses in 2D vs slice culture and flank versus intracranial slice cultures	184
Pressurized in vitro circulating tumour cell culture platform	Pressure control	Doxorubicin resistance can be increased under high pressure culture condition through ABCC1 overexpression	194
Lung on a chip with electrospun membrane	Co-culture of NSCLC cell and fibroblasts; Shear stress control	IGF-1 secretion by HFL1 cells activates the PI3K/Akt pathway in A549 cells which promotes gefitinib resistance	76
Flexible lung alveolus chip	Co-culture of NSCLC, normal lung alveolar epithelial cells and lung endothelial cells; Cyclic strain control	Increased resistance to the third-generation tyrosine kinase inhibitor, rociletinib, mediated by mechanical strain-induced changes in EGFR phosphorylation	195
3D chamber seeded with A549 lung cancer cells connected to a chamber seeded with CAFs, with a concentration gradient generator	Co-culture; Nutrient gradient control	Production of HGF by CAFs inhibits paclitaxel-induced apoptosis in lung cancer cells	196
SERS nanosensors mapping redox potential and pH in 3D tumour spheroids	Real-time monitor; 3D mapping of redox potential and pH gradients	Monitoring apoptosis and drug resistance via changes in the redox potential gradients in the spheroids	121

RT-PCR: Reverse transcription-polymerase chain reaction. EpCAM: Epithelial cell adhesion molecule. SYL3C: Anti- EpCAM aptamer. CXCL12: Chemokine stromal cell-derived factor 1. CXCR4: C-X-C chemokine receptor type 4. PHT-427: Dual Akt and PDPK1 inhibitor, NSCLC: Non-small cell lung cancer, EGFR: epidermal growth factor receptor, SERS: Surface enhanced Raman spectroscopy. CAF: cancer-associated fibroblast, HGF: hepatocyte growth factor, ROS : reactive oxygen species.

Table 2 |

Nanosensors categorized based on base material Sensor design Signal Instrumentatio Target Advantage Limitation

Sensor design	Signal transduction	Instrumentation	Target	Advantage	Limitation
Single-walled carbon nanotube (SWCNT)					
Conjugation of actuators	Solvatochromic effect-induced fluorescence intensity and/or wavelength change	NIR fluorescence spectrometer and microscopy	miRNAs[182]; Proteins[103,183]	Biocompatibility NIR-II emission Photostability	Low quantum yield (1–20% in aqueous media); Possibility of low selectivity in molecular-recognition-based sensors for *in vivo* use.
Polymer wrapping			Proteins[153]; Metabolites[153,154]. RoS[99–101]; Lipids[107,147]		
Incorporation of fluorescent quantum defects			Proteins[186,197]; pH[198]		
Metallic nanoparticle					
Conjugation of actuators to plasmonic nanoparticle	Vibrational fingerprint in SERS spectra	Raman microscopy; Optical nanopipette	pH[119–121,159]; ROS[160]; Redox potential[121]	Flexible excitation wavelength Photostability	Invasive implementation of probe tip
Conjugation of actuators to quantum dot or metal oxide	FRET-based intensity modulation	Visible/NIR fluorescence spectrometer and microscopy	pH[110,111]; ROS[104]; Protease activity[110]	Tunable photophysicochemical properties Structure versatility High quantum yield High chemical stability	Photobleaching Potential cytotoxicity in long-term *in vivo* use
Polymeric nanoparticle					
Encapsulation or covalent conjugation of actuators to polymers	Fluorescence intensity change; Chemiluminescence	Visible and NIR fluorescence spectrometer and microscopy	pH[108,109,112]; Protease activity[199]; ROS[166]; Oxygen levels[106]	Broad functional tunability; Biocompatibility	Dearth of robust NIR-II dyes; Irreversible disassembly-based signal activation
Radiolabelled nanoparticles					
Conjugation of actuators to radiolabelled inorganic nanoparticles or peptides	PET imaging	PET scanner	Proteins[161]; Immune cells[161]	Picomolar range sensitivity; Whole body imaging capability; Non-invasive; Multimodal imaging capability[200]	Expensive instrumentation
Electrochemical probe					
Conjugation of actuators to probe	Electrical impedance change by target analytes	Amperometric nanopipette	Proteins[164]; Metabolites[136,137]; Glucose[127,128 137]	High sensitivity Fast response time Integration in a 2D or 3D array platform for high-throughput sensing[201]	Invasive implementation of probe tip; Localized measurement

FRET: Förster resonance energy transfer. miRNAs: microRNAs. NIR: near infrared. SERS: Surface enhanced Raman spectroscopy. PET: Positron emission tomography. ROS: reactive oxygen species.